comp

1080

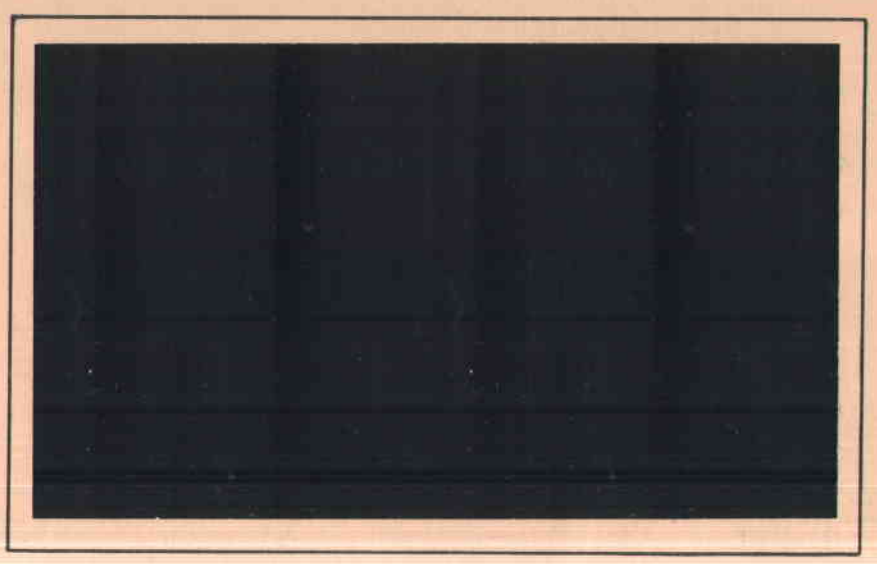

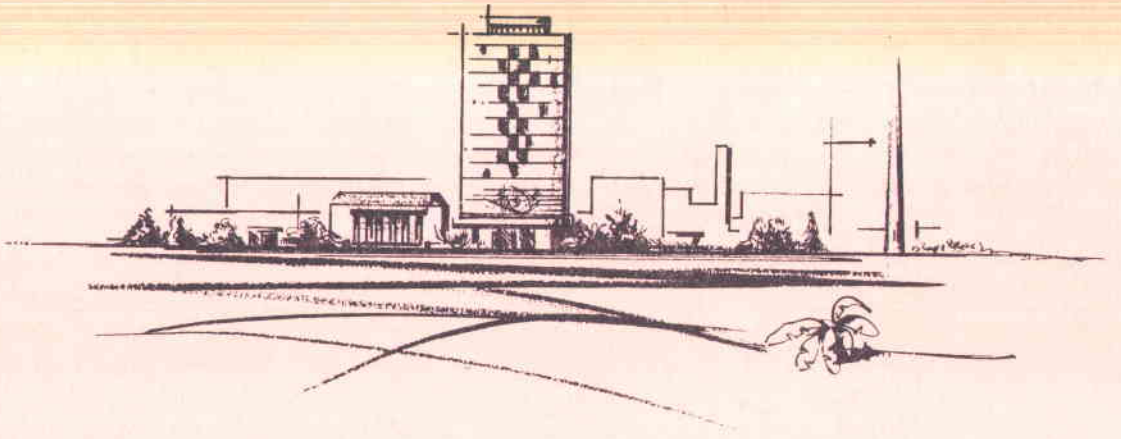

BATTELLE MEMORIAL INSTITUTE

COLUMBUS LABORATORIES

BATTELLE MEMORIAL INSTITUTE

COLUMBUS LABORATORIES • 505 KING AVENUE • COLUMBUS, OHIO 43201

DEDICATED TO THE ADVANCEMENT OF SCIENCE

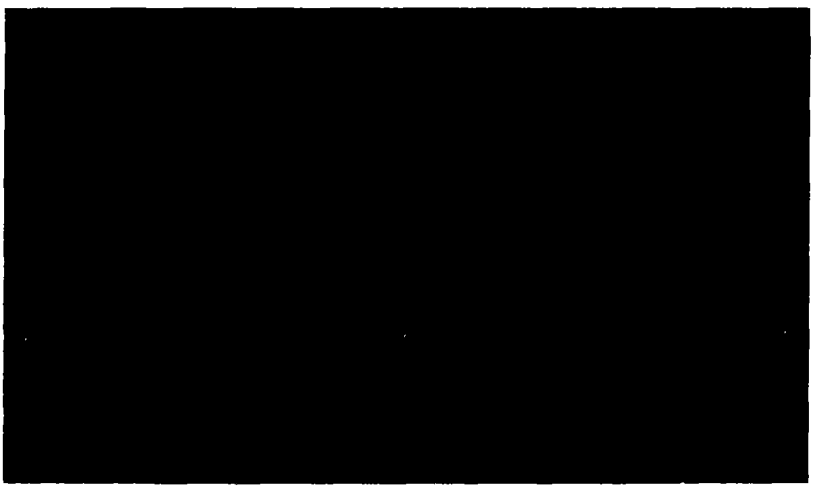

FIELDS OF RESEARCH

Aeronautics — Astronautics
Agricultural Chemistry
Agricultural Economics
Alloy Development
Applied Mathematics
Area Economics
Biochemistry
Biophysics — Bionics
Catalysis — Surface Chemistry
Ceramics
Chemical Engineering
Chemical Processes
Communications Science
Computer Technology
Corrosion Technology
Earth — Atmospheric Sciences
Electrochemistry
Electronics
Energy Conversion
Engineering — Structural Materials
Environmental Systems
Extractive Metallurgy
Extreme-Temperature Technology
Ferrous Metallurgy
Food Technology
Foundry Practice
Fuels — Combustion
Glass Technology
Graphic Arts Technology
Immunology — Cancer Studies
Industrial Economics
Industrial Physics
Information Research
Inorganic Chemistry
Instrumentation
Light Alloys — Rare Metals
Lubricant Technology
Materials Separation — Concentration
Mechanical Engineering
Metal Fabrication Engineering
Metal Finishing
Metallurgical Processes
Microbiology
Microscopy — Mineralogy
Nondestructive Evaluation Technology
Nonferrous Metallurgy
Nucleonics
Ocean Engineering
Organic Chemistry
Organic Coatings
Packaging Research
Particle Dynamics
Petrochemicals
Petroleum Engineering
Pharmaceutical Chemistry
Physical Chemistry
Production Engineering
Psychological Sciences
Pulp — Paper Technology
Radioisotopes — Radiation
Reactor Technology
Refractories
Reliability Engineering
Rubber — Plastics
Semiconductors — Solid-State Devices
Sound — Vibration
Systems Engineering
Textiles — Fibers
Theoretical — Applied Mechanics
Thermodynamics
Transportation
Welding — Metals-Joining Technology
Wood — Forest Products

HEAT-PIPE ANALYSIS, FABRICATION, AND EVALUATION CAPABILITIES

Materials Systems Engineering Division
Materials Development Division

BATTELLE MEMORIAL INSTITUTE
Columbus Laboratories

TABLE OF CONTENTS

INTRODUCTION TO HEAT PIPE
THEORY AND PERFORMANCE

INTRODUCTION

The heat pipe is a relaively recent development (1964) in extremely efficient heat-transport devices. The basic phenomena of evaporation, condensation, and surface tension pumping within a capillary wick structure permit the heat pipe to transfer large quantities of heat without the use of external components. Because the heat pipe can operate without the aid of condensate-return pumps, gravity, or centrifugal-force fields, it differs from conventional boiling-condensing thermal systems (e.g., Rankine cycle or reflux condenser systems). Theoretically, the heat pipe can transfer up to 500 times as much thermal energy per unit weight as can a solid thermal conductor having the same cross section. By appropriate selection of working fluids, heat pipes have been designed and operated at temperatures ranging from the cryogenic temperatures up to 2250 K (3590 F) and are limited at higher temperatures by available materials' technology.

Operationally, the heat pipe can be characterized as being simple, relatively inexpensive, and capable of operating silently and reliably for long lifetimes. Thermal energy may be transferred to or from the heat pipe by radiation, convection, or conduction, and it may be used with a variety of energy sources such as open flames, electric heaters, solar radiation, or nuclear sources. Because it has a fraction of the weight and has several hundred times the heat-transfer capability of copper, silver, or aluminum, the heat pipe can replace, or supplement, many conventional heat-transfer systems relying on thermal conduction coupling.

Typically, heat pipes are built from circular-cross-section tubes such as is shown in Figure 1. The structural elements of the heat pipe are a closed outer vessel, a porous capillary wick, and a working fluid. The wick is normally held uniformly against the inside wall of the pipe. Glass or metal tubes may be used for the gas-tight containment vessel. Demonstrated working fluids include water, acetone, alcohol, glycerine, ammonia, Freon, molten salts, and molten metals, including Hg, Na, and Li. Typical wick materials are woven cloth, fiberglass, porous metal, wire screen, porous ceramic tube, narrow grooves cut lengthwise in the pipe wall, and corrugated or perforated metal sheet.

As shown in Figure 1, heating one region of the heat pipe evaporates working fluid from the wick and drives the vapor to other regions where it condenses, giving up the latent heat of vaporization. It is this phase change which gives rise to the high thermal performance of the heat pipe. Within the wick, capillary forces return the condensate back to the evaporator region. Typical heat-pipe operation is characterized by very nearly isothermal conditions along its length. A small-temperature gradient exists because a small-vapor-pressure gradient is generated between the evaporator and condenser sections and because there are some radial temperature gradients due to thermal conduction where thermal energy is added and removed. The pressure within the heat pipe is the saturation vapor pressure corresponding to the operating temperature condition. The operating temperature in turn is a function of the heat sink temperature and method of attachment.

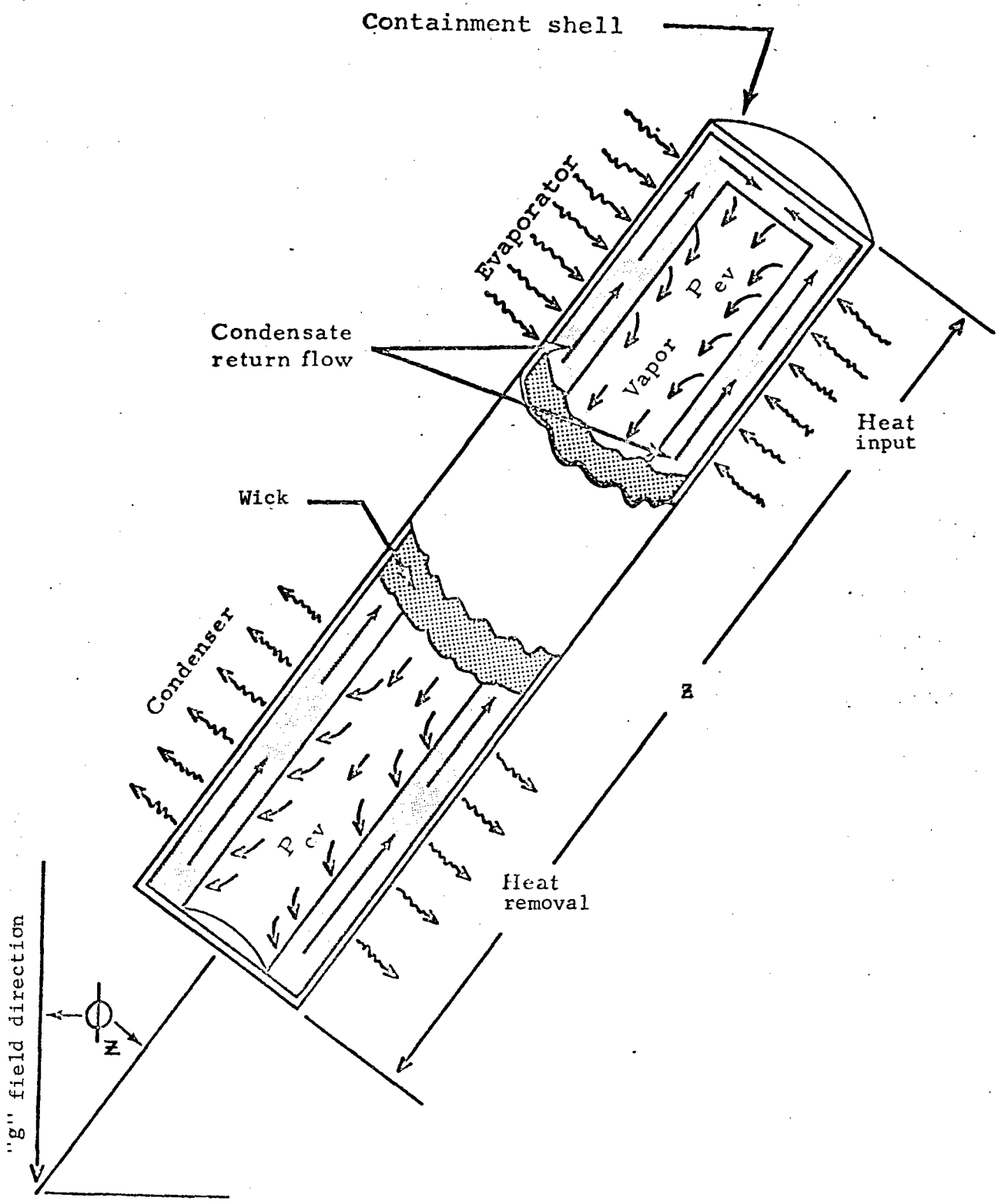

FIGURE 1. OPERATING HEAT PIPE

In order to be an effective heat transfer device, the heat pipe must be optimized to properly merge the physical characteristics of the working fluid with the geometric constraints and the desired operational temperature range. The maximum thermal power per unit temperature difference (between the extreme end points of the heat pipe) that can be transferred in a heat pipe of fixed dimensions, is determined by

(1) The pumping capability of the wick structures

(2) The thermophysical properties (particularly the thermal conductivity) of the materials of construction employed for the wick and containment vessel and methods of attachment (i.e., thermal impedances between shell and wick in the evaporator and condenser sections)

(3) The physical properties of the working fluid (viz., surface tension, contact angle, latent heat of vaporization, viscosity of the liquid and gas phases, density of the liquid and gas phases, vapor pressure) over the temperature range of interest

(4) The onset of boiling of the fluid in the evaporator regions, due to superheating of the fluid induced by high heat fluxes

(5) The onset of entrainment, i.e., the counterflow shear between the liquid (on the wick) and the vapor (in the vapor passage) phases

(6) The vapor phase sonic limit, i.e., the "upper-limit" velocity at which vapor can be transferred from the evaporator to the condenser regions of the heat pipe.

Figure 2 schematically relates those parameters of importance to the three major regions of a cylindrical heat pipe.

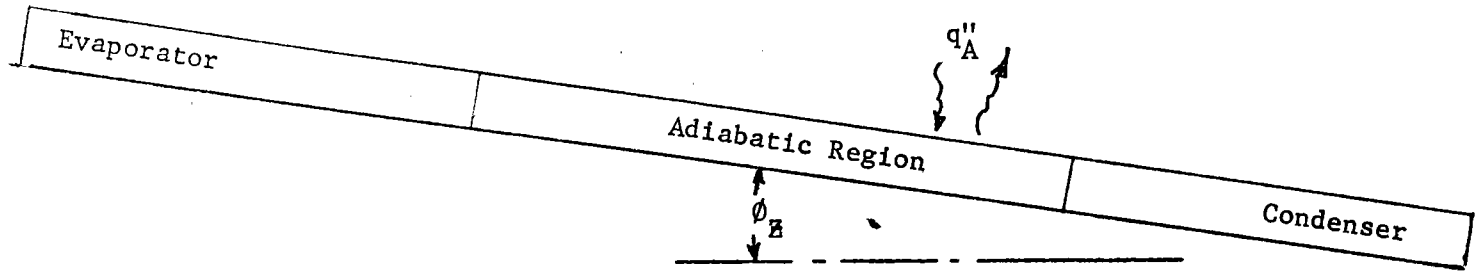

Evaporator Region

- Input heat flux (q''_E)
- Wick effective pore radius (r_{P_E})
- Fluid wetting angle (θ_E)
- Surface tension (σ)
- Heat of vaporization (ΔH_{fg})
- Temperature differentials (ΔT_E)
- Working fluid density (ρ_l, ρ_v)
- Working fluid viscosity (μ_l, μ_v)
- Fluid and wick thermal conductivity (k_f, k_w)

Adiabatic Length

- Effective pore size (r_{P_A})
- Free flow area (A_{ff_A})
- Effective flow length (L_{A_e})
- μ_l, ρ_l
- Parasitic heat losses/additions (q''_A)
- Gravity or inertial forces
- Attitude angle, ϕ_z

Condenser Region

- Condenser heat flux (q''_e)
- Wick effective pore size (r_{P_c})
- θ_E, σ, ΔH_{fg}
- Temperature differentials to heat sink (ΔT_c)
- ρe, ρv, μe, μv
- Fluid and wick thermal Conductivity (h_f, h_w)

FIGURE 2. DESIGN PARAMETERS VERSUS HEAT PIPE LOCATION

THEORETICAL ANALYSIS

Several derivations of the heat-pipe maximum heat-transfer rate and associated optimization techniques have been reported in the literature. Consider the heat pipe shown in Figure 1. When operating at steady-state conditions, the sum of the pressure changes in the closed-cycle system may be described by the following equation:

$$\underbrace{\Delta p_\sigma}_{\text{Liquid surface tension pumping in wick}} \geq \underbrace{\Delta p_g}_{\text{Gravitational field effect}} + \underbrace{\Delta p_\ell}_{\text{Viscous flow losses in wick}} + \underbrace{\Delta p_v}_{\text{Viscous flow losses in vapor}} . \quad (1)$$

The heat pipe can operate without drying out the wick so long as the pumping pressure term is greater than or equal to the pressure losses in the liquid and the vapor, and those due to gravitational or acceleration field effects (which may either help, hinder, or be nonexistent).

WICK SELECTION

The wick structure performs the following four basic functions: (1) liquid pumping - results from surface tension forces developed in wick pores at the liquid-vapor interface, small pores are desirable, particularly in the evaporator region; (2) liquid-flow path - liquid drawn from the condenser to the evaporator flows in wick channels, large, smooth wall channels are desirable for low hydrodynamic losses; (3) radial heat-flow path - thermal energy required for evaporation is transferred through liquid-wick composite structure, high thermal conductivity of both wick and liquid is desirable; and (4) liquid vapor-flow separation - at high-performance conditions, the counterflow shear between the liquid and vapor phases becomes important, fine pores or even a solid separation layer is desirable at the liquid-vapor interface in the midsections of high-performance heat pipes. In addition, the wick must also be made of a material which is chemically and metallurgically compatible with the working fluid and containment vessel, it must be manufacturable, and, depending on application, it may need to be a dielectric material.

WORKING FLUID SELECTION

In choosing a heat-pipe working fluid for a given temperature range, the following factors need to be considered. The vapor pressure of the working fluid should not be so high that the heat pipe must become a pressure vessel with prohibitively thick walls. However, the slope of the vapor pressure-versus-temperature curve should be large so that small differences in temperature between the evaporator and condenser regions of the heat pipe will provide large differences in the pressure of the vapor. A fluid having a high latent heat is desirable in order to transfer the maximum amount of heat with the minimum flow of fluid. A high thermal conductivity of the liquid minimizes radial temperature differences across the liquid layer in the evaporator wick section and reduces the possibility of localized boiling at the container wall-to-wick interface. The viscosity of both the liquid and vapor should be low in order to minimize the resistance to fluid circulation. The flow of liquid in the wick structure depends upon capillary action and, therefore, a fluid having a high surface tension is desired. Similarly, the wick structure must be completely "wetted" by the liquid in order for the capillary action to function properly.

As mentioned under "wick selection", there must not be any appreciable chemical or metallurgical reaction between the working fluid and the wick or the heat-pipe containment vessel. For example, the use of water in an aluminum heat pipe results in a chemical reaction which generates hydrogen and which is swept into the condenser in the form of a noncondensable gas and, consequently, interferes with the operation of the heat pipe in that region. Any reactions which could alter the fluid properties are undesirable.

LIMITS OF OPERATION

The heat pipe possesses heat-transfer limitations which are governed by certain principles of fluid mechanics. The possible effects of these limitations on the capability of a heat pipe are shown in Figure 3. The relative magnitudes of each of these limitations will vary depending on heat-pipe geometry, working fluid, and wick characteristics. The individual limitations indicated in the figure are discussed below.

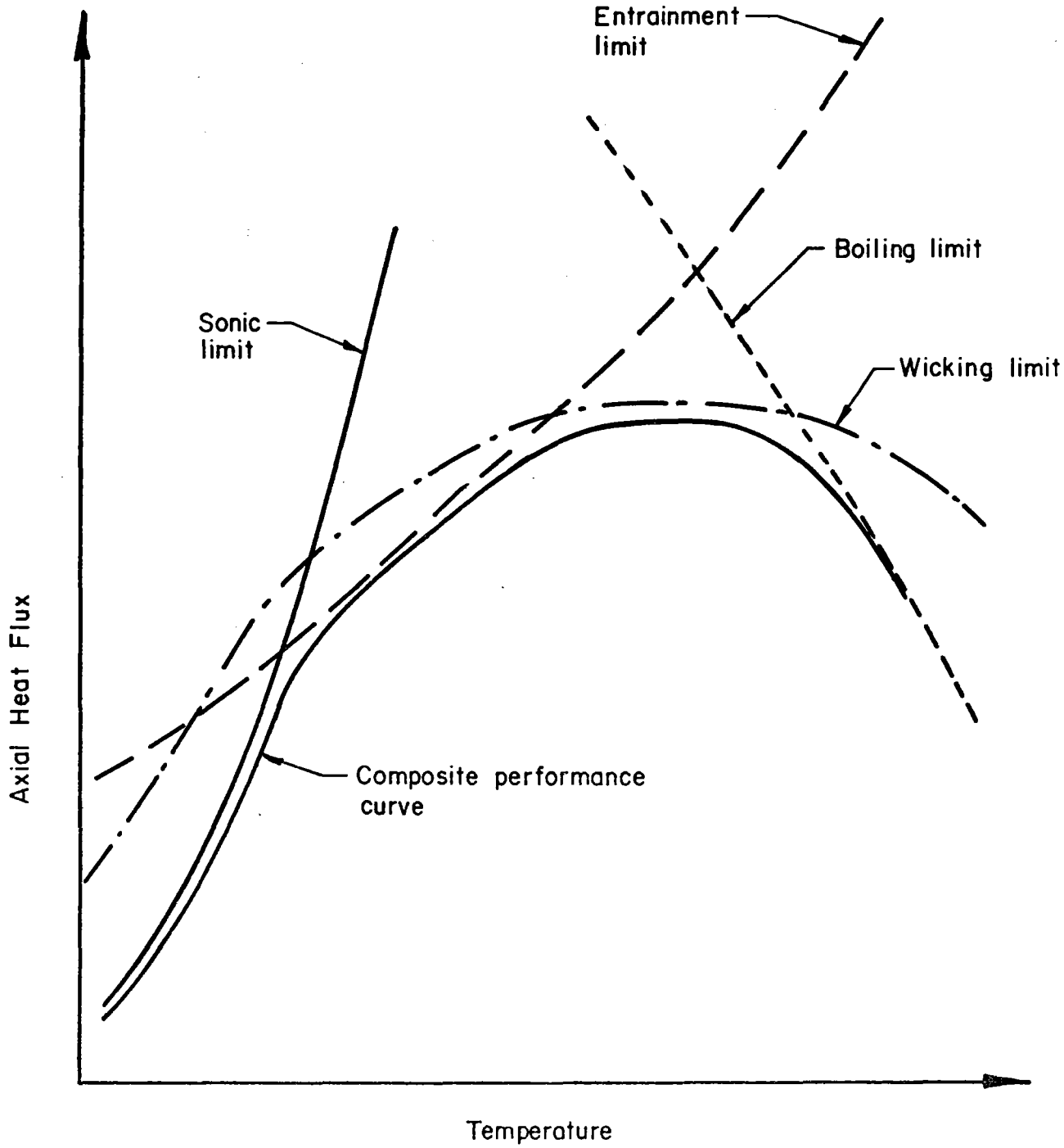

FIGURE 3. HEAT-PIPE OPERATING LIMITS

Sonic Limit

The rate of heat transfer, Q, from the evaporator section of the heat pipe to the condenser section is given by:

$$Q = \dot{m}_v L \quad , \tag{2}$$

where $\dot{m}_v$ is the rate of mass flow of vapor at the evaporator exit, and L is the latent heat of the fluid. Since the latent heat of the working fluid is used instead of its heat capacity, rather large heat-transfer rates can be achieved with a relatively small mass flow. Furthermore, if the heat is transferred by high-density, low-velocity vapor, the transfer is nearly isothermal because small pressure gradients in the vapor support its motion.

The above equation can be used to show the effect of vapor density and velocity on heat transfer by using the continuity equation:

$$\dot{m}_v = \bar{\rho}_v \bar{V} A \quad , \tag{3}$$

where $\bar{\rho}_v$ is the radial average vapor density at evaporator exit, $\bar{V}$ is the average axial vapor velocity at evaporator exit, and A is the cross-sectional area of the vapor passage. The combination of Equations (2) and (3) obtains:

$$Q/A = \bar{\rho}_v \bar{V} L \quad , \tag{4}$$

where Q/A is the axial heat flux based on the cross-sectional area of the vapor passage. According to Equation (4), the axial heat flux in a heat pipe can be held constant and the condenser environment adjusted to lower the pressure, temperature, and density of the vapor until the flow at the evaporator becomes sonic. This sonic limiting condition is represented in Figure 3. Typical values of sonic heat-flux limits for Cs, K, Na, and Li are 37.3 (at 700 C), 36.6 (at 700 C), 94.2 (at 900 C), and 143.8 (at 1300 C) kw/cm^2.

Entrainment Limit

The sonic limitations discussed above do not ordinarily cause dryout of the wick with attendant overheating of the evaporator. Rather, they often prevent the attainment of other limitations during startup. However, if the vapor density is allowed to increase without an accompanying

decrease in velocity, some liquid from the wick-return system may be entrained. The onset of entrainment can be expressed in terms of a Weber number:

$$\frac{\rho_v V^2 \lambda}{2\pi \gamma} = 1 \quad , \tag{5}$$

where λ is a characteristic length and γ is the surface tension. This equation expresses the ratio of vapor inertial forces to liquid surface tension forces. When this ratio exceeds unity, entrainment begins and the fluid circulation increases until the liquid-return path cannot accommodate the increased flow. This results in dryout of the wick and overheating of the evaporator.

Since the wavelength of the perturbations at the liquid-vapor interface in a heat pipe is determined by the wick structure, the entrainment limit can be estimated by combining Equations (4) and (5) to give:

$$Q/A = \sqrt{\frac{2\pi \rho_v \gamma L^2}{\lambda}} \quad . \tag{6}$$

The above equation can then be used to obtain the type of "entrainment limit" curve represented in Figure 3.

Wicking Limit

The circulation of the working fluid in a heat pipe is maintained by capillary forces which develop in the wick structure at the liquid-vapor interface. These forces balance the pressure losses due to the flow in the liquid and vapor phases and are manifest as many tiny menisci which allow the pressure in the vapor to be higher than the pressure in the adjacent liquid in all parts of the system. A typical meniscus is characterized by two principal radii of curvature (r_1 and r_2) and the pressure drop, Δp_σ, across the liquid surface is given by:

$$\Delta p_\sigma = \gamma \left(\frac{1}{r_1} + \frac{1}{r_2}\right) \quad . \tag{7}$$

These radii, which are smallest at the evaporator end of the heat pipe, become even smaller as the heat-transfer rate is increased. If the liquid wets the wick perfectly, the radii will be defined exactly by the pore size of the wick when a heat-transfer limit is reached. Any further increase in heat transfer will cause the liquid to retreat into the wick, and drying and overheating will occur at the evaporator end of the system.

The capillary force in a heat pipe can be increased by decreasing the size of the wick pores which are exposed to vapor flow. However, if the pore size is decreased also in the remainder of the wick, the wicking limit might actually be reduced because of the increased pressure drop in the liquid phase. This is shown by Poiseuille's equation for the pressure drop through a capillary tube:

$$\Delta p_{\ell} = \frac{8\mu \dot{m}_{\ell} Z}{\pi r^4 \rho} , \tag{8}$$

where μ is the liquid viscosity, $\dot{m}_{\ell}$ is the mass rate of flow of liquid, r is the effective radius of the capillary tube, ρ is the liquid density, and Z is the capillary tube length.

The above equation can then be used to calculate the liquid-pressure drop at a particular heat-transfer rate, Q, for various wick structures. The geometry factors associated with various wick structures are reported in the literature.* An example of a wicking limitation curve is shown in Figure 3.

Boiling Limit

In most two-phase flow systems, the formation of vapor bubbles in the liquid phase (boiling) enhances convection, which is required for the heat transfer. Such boiling is difficult to achieve in liquid-metal systems because the liquid tends to fill the nucleation sites necessary for bubble formation. In a heat pipe, convection in the liquid is not required because heat enters the pipe by conduction through a thin, saturated wick. Furthermore, the formation of vapor bubbles is undesirable because they could cause hot spots and interrupt the action of the wick. Therefore, heat pipes are usually heated isothermally in order to facilitate the wetting of the inner heat-pipe wall and the filling of all but the smallest nucleation sites.

Since the sizes of nucleation sites in any system are difficult to predict, it is not possible to predict when and where boiling will occur. However, the following two equations do indicate how various factors influence boiling:

$$P_i - P_{\ell} = \frac{2\gamma}{r} ,$$

$$\frac{Q}{S} = \frac{k(T_w - T_v)}{t} ,$$

---

* Cheung, H., "A Critical Review of Heat Pipe Theory and Applications", Report No. UCRL-50453, Lawrence Radiation Laboratory (July 15, 1968).

where P_i is vapor pressure inside bubble, P_ℓ is pressure in adjacent liquid, r is radius of largest nucleation sight, S is heat input area, k is effective thermal conductivity of saturated wick, T_w is temperature at inside wall, T_v is temperature at liquid-vapor interface, and t is wick thickness. As an example, if H_2O is used as the working fluid, boiling often becomes the major heat-transfer limitation because the thermal conductivity is low and because the liquid phase does not readily fill nucleation sites. The boiling limitation usually occurs only in nonmetal working fluids and typically at high input heat fluxes and high operating temperatures as shown in Figure 3.

SUMMARY OF PERFORMANCE FOR SELECTED WORKING FLUIDS

SUMMARY OF HEAT PIPE PERFORMANCE

The maximum heat transfer capability parameter, $\sigma\Delta H\sqrt{\frac{\rho_l}{\mu_l}\cdot\frac{\rho_v}{\mu_v}}$, which can be calculated from fluid property data is often employed for preliminary fluid selection. Table 1 summarizes this parameter for typical fluids which could be (and some have been) employed in heat pipes. Table 2 contains property data for selected heat pipe working fluids.

A summary of attained heat-pipe performance which has been reported for a variety of working fluids is shown in Table 3. It is readily apparent from this table that little experimental data are available for heat-pipe operation in the near-room-temperature regime or below. One trend evident from this table is the significant decrease of axial heat-flux capability with decreasing heat-pipe operating temperatures. Also, higher internal pressures are required for the effective operation of heat pipes in the low-temperature regimes (70 to 400 K; -335 to 260 F).

TABLE 1. MAXIMUM HEAT-TRANSFER CAPABILITY OF SELECTED HEAT-PIPE WORKING FLUIDS

Material	Temperature, F	Saturation Pressure, psia	$\sigma \cdot \Delta H_v \sqrt{\frac{\rho_\ell}{\mu_\ell} \cdot \frac{\rho_v}{\mu_v}}$, Btu/(sec)(ft^2)
		Nonmetals	
N_2	-333.7	5.60	2.63×10^5
O_2	-333.7	0.91	5.28×10^5
NH_3 (Ammonia)	0	30.42	27.3×10^5
	50	89.19	39.75×10^5
	100	211.9	45.8×10^5
H_2O (Water)	50	0.18	4.57×10^5
	100	0.95	11.65×10^5
	150	3.72	24.3×10^5
	200	11.53	43.2×10^5
	400	247.0	97.0×10^5
$CHCl_2F$ (Freon-21)	0	4.58	3.08×10^5
	50	15.33	5.18×10^5
	100	40.04	7.93×10^5
	150	87.51	11.09×10^5
Isopentane	100	--	2.3×10^5
		Metals	
Sodium	900	.04	28.3×10^5
	1200	1.00	88.5×10^5
	1500	7.00	$220. \times 10^5$
	1800	33.0	$314. \times 10^5$

TABLE 2. PROPERTIES OF SELECTED HEAT-PIPE WORKING FLUIDS

Substance	Freezing Point, F	Temperature, F	Saturation Pressure, psia	ΔH_{fg}, Btu/lb_m	ρ_ℓ, lb_m/ft^3	ρ_v, lb_m/ft^3	Centipoises μ_ℓ	Centipoises μ_v	σ, dynes/cm
				Nonmetals					
N_2		-333.7	5.60	88.3	46.4	0.1965	0.230	0.00517	10.6
O_2		-333.7	0.91	99.2	77.5	0.2200	0.395	0.00503	17.9
NH_3	-108	0	30.42	568.9	41.4	0.109	0.195	0.00865	--
		50	89.19	527.3	39.1	0.304	0.130	0.0095	23.4 at 11.1 C
		100	211.9	477.8	36.4	0.705	0.0925	0.0106	18.1 at 34.1 C
		174	560.0	--	--	--	--	--	--
H_2O	+32	50	0.178	1065.6	62.4	0.000587	1.25	0.0091	73
		100	0.949	1037.2	62.0	0.00286	0.725	0.0101	69.6
		150	3.718	1008.2	61.3	0.0103	0.46	0.0111	66.0
		200	11.526	977.9	60.15	0.02975	0.290	0.0121	57
		400	247.0	825.0	53.5	0.5400	0.135	0.0176	33.3
Freon-21	-211	0	4.582	109.93	91.5	0.0968	0.49	0.0100	24.4
		50	15.33	103.90	87.7	0.291	0.40	0.0108	20.0
		100	40.04	97.11	83.3	0.729	0.34	0.0115	16.3
		150	87.51	89.06	78.8	1.546	0.28	0.0121	13.1
				Metals					
Sodium	208 F	900	.04	1840	51.7	8.0×10^{-5}	.25	.00176	155.
		1200	1.00	1770	49.2	1.03×10^{-3}	.20	.00199	137.
		1500	7.00	1690	47.2	9.0×10^{-3}	.165	.0022	118.
		1800	33.0	1625	45.1	2.5×10^{-2}	.14	.0024	103.

TABLE 3. SUMMARY OF HEAT-PIPE PERFORMANCE FOR VARIOUS WORKING FLUIDS

Working Fluid	Practical Temperature Range	Measured Axial Heat Flux*	Fluid-Vapor Pressure
(1) Liquid nitrogen	70 to 120 K (-330 to -240 F)	40 watts/cm^2 at 78 K	~300 psia at 120 K
(2) Water	300 to 500 K (80 to 440 F)	390 watts/cm^2 at 400 K	~300 psia at 490 K
(3) Mercury	460 to 820 K (370 to 1020 F)	1000 watts/cm^2 at 800 K	~200 psia at 800 K
(4) Potassium	675 to 1075 K (780 to 1480 F)	870 watts/cm^2 at 1075 K	~20 psia at 1075 K
(5) Sodium	775 to 1175 K (940 to 1660 F)	1400 watts/cm^2 at 1175 K	~20 psia at 1175 K
(6) Lithium	1175 to 1775 K (1660 to 2740 F)	1950 watts/cm^2 at 1520 K	~25 psia at 1775 K
(7) Silver	1775 to 2275 K (2740 to 3640 F)	4000 watts/cm^2 at 2025 K	~15 psia at 2275 K

* Heat pipe operating in horizontal position.

HEAT-PIPE THEORETICAL ANALYSIS CAPABILITY

DESCRIPTION OF HEAT-PIPE COMPUTER PROGRAM

A computer program developed at BCL for the design and prediction of heat-pipe performance is described below. The digital computer program calculates performance based on fixed geometries as well as performs design optimization as a function of:

(1) Maximum heat-flux capability

(2) Optimum pore size within the wick

(3) Operational temperature requirements.

The heat-pipe performance calculations are based on the physical model shown in Figure 4 and can accommodate heat-pipe designs having:

(1) Arbitrary diameters of principal heat-pipe components (i.e., wick, vapor passage, sleeve, etc.)

(2) Arbitrary lengths for the three principal regions (i.e., evaporator adiabatic length, and condenser).

On the basis of the analytical model shown in Figure 4, the computer program logic provides for the acceptance of variable input data, design and optimization computations, and tabulation of output data. Generalization has been achieved by providing for (as part of the input data section) the majority of conceivable design parameters.

The program inputs include the following parameters:

(1) Properties of working fluid (latent heat of vaporization, viscosity, vapor pressure, density, contact angles of fluid in capillary voids, surface tension of fluid, and ratio of specific heats of liquid and vapor phases either as constants or as a function of temperature)

(2) Properties of heat-pipe components (thermal conductivity, density, pore radius, pressure-drop factors associated with liquid flow in a capillary structure)

(3) Dimensions of heat-pipe components (radius of sleeve, container, wick, and vapor passage; lengths of evaporator, adiabatic, and condenser regions)

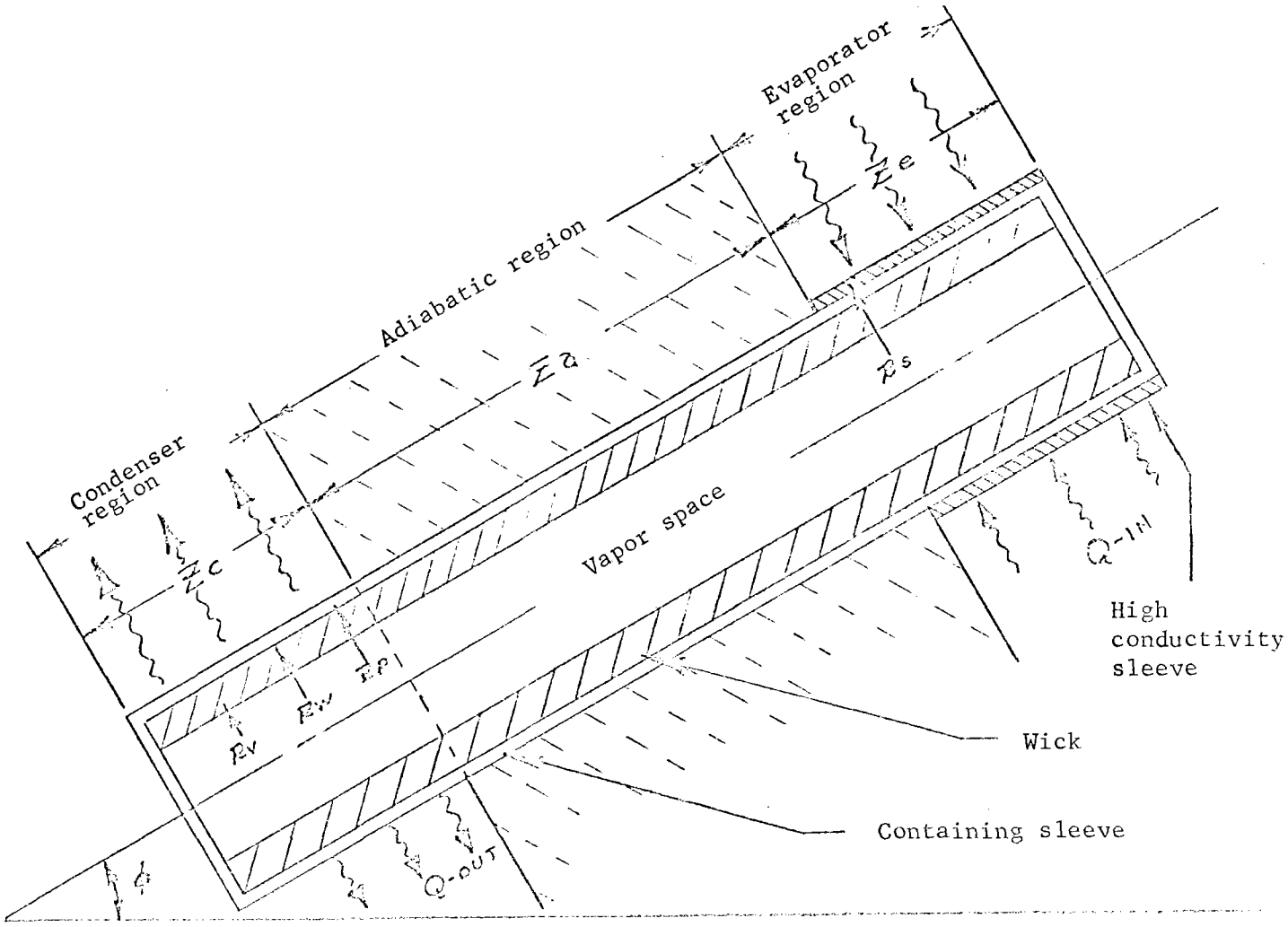

FIGURE 4. ANALYTICAL MODEL FOR HEAT-PIPE ANALYSIS

(4) Attitude of heat pipe relative to gravitational force vector

(5) Numerical factor in condensation rate equation (i.e., "sticking coefficient")

(6) Range of operating temperatures for heat pipe

(7) Heat-flux requirement (optional).

The temperature-dependent properties used in the analysis are expressed in terms of a polynomial equation in order to facilitate rapid computation of performance parameters over a wide range of temperatures.

The computational scheme of the computer program is illustrated by the flow chart shown in Figure 5. Several optional calculational schemes are available for the heat-pipe analysis which permit (1) the optimization of the heat-pipe design with respect to maximum heat-flux capability--based on fixed properties for the heat-pipe components, fixed overall diameter of heat pipe, and fixed length of each region of heat pipe: (2) the sizing of the effective "pore radius" of the wick--based on fixed properties of the heat-pipe components, fixed dimensions of each of the components, fixed heat-flux capacity, and fixed operating temperature; and (3) the computation of the maximum heat-flux capability--based on fixed properties of the heat-pipe components, fixed dimensions of each of the components, fixed "pore radius" of the wick, and fixed operating temperature.

The program output lists the following parameters:

(1) Optimum wick pore size for vapor flowing in the laminar and turbulent flow regimes

(2) Maximum heat-flux capability of given heat-pipe design as a function of heat-pipe attitude and operating temperature

(3) Radial and axial Reynolds numbers associated with each of the three regions of the heat pipe as a function of temperature

(4) Radial temperature difference across heat pipe (due to conductive heat transfer through sleeve, container, and wick) as a function of operating temperature

(5) Maximum effective operational length of heat pipe as a function of attitude and operating temperature.

In addition to the performance controlling parameters listed above, the BCL heat-pipe design program includes provisions for (1) analysis of both turbulent and laminar (axial and radial) flow regimes in the vapor "space" of the heat pipe and (2) treating either compressible or incompressible vapor flow within the evaporator section of the heat pipe. This latter

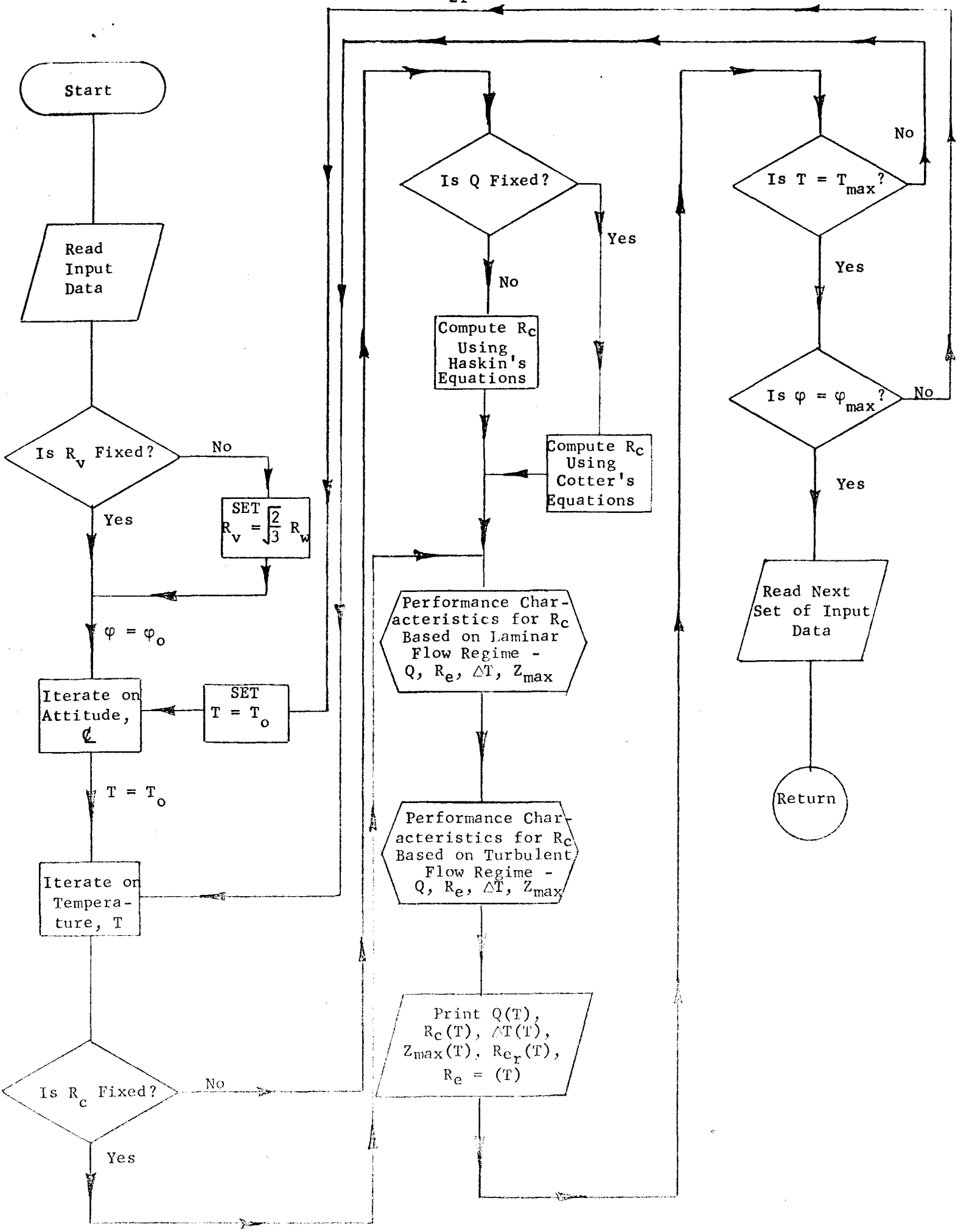

FIGURE 5. FLOW CHART FOR HEAT-PIPE COMPUTER PROGRAM

consideration is a refinement to the present theory of heat pipes since it can be shown that the incompressible theory yields a conservatively low prediction of the heat flux since the pressure recovery in the condenser is higher when compressibility is taken into account. The effect of compressibility is particularly important during the startup transient and for operation at low temperatures and/or vapor pressures. These design and performance analyses are supplemented as required by detailed analytics carried out via other generalized heat transfer/fluid dynamics computer codes such as CINDA-3G, THT-D and TRUMP, all of which are operational at Battelle-Columbus.

HEAT-PIPE WICK FABRICATION CAPABILITIES

WICK STRUCTURE REQUIREMENTS

The key component of a high performance heat pipe is the wick structure. The availability of wick structures, or the fabrication capability, will be the most significant factor in the successful development of the heat pipes cryogenic heat pipe. Basically, the wick structure must perform the following four functions:

(1) Liquid pumping - results from surface tension forces developed in wick pores at the liquid-vapor interface, small pores are desirable, particularly in the evaporator region

(2) Liquid-flow path - liquid drawn from the condenser to the evaporator flows in wick channels, large, smooth wall channels are desirable for low hydrodynamic losses

(3) Radial heat-flow path - thermal energy required for evaporation is transferred through liquid-wick composite structure, high thermal conductivity of both wick and liquid is desirable

(4) Liquid/vapor flow separation - at high-performance conditions, the counterflow shear between the liquid and vapor phases becomes important, fine pores or even a solid separation layer is desirable at the liquid-vapor interface in the adiabatic regions of high-performance heat pipes.

The large variability of surface tension characteristics of potential working fluids (i.e., cryogens $\simeq$ 8 dynes/cm; water $\simeq$ 76 dynes/cm; liquid metals $\simeq$ 150 dynes/cm) require a flexible, comprehensive fabrication capability which can reproduce wick structures cheaply if these are not available commercially. The materials fabrication capabilities of BCL which could be made available for the development of wick structures for a wide range of heat pipes are described next.

Controlled Porosity Structures

BCL has produced many controlled porosity components through powder metallurgy (P/M) methods. These experimental components have been fabricated from a wide variety of materials (e.g., tungsten, titanium, stainlees steel, nickel, copper, et al). The fabrication technique employed to fabricate these porous structures varies with the specific situation and depends upon the materials, pore size, pore size distribution, pore shape, pore volume, components geometry, microstructure, purity, and mechanical properties, required in the final product. Economic considerations are employed to

choose the best fabrication technique among those techniques which produce acceptable components. The powder metallurgy techniques commonly employed by BCL include: (1) pressureless sintering or irregular and/or spherical powders, (2) pressureless sintering or a hydropressed or die pressed preform, (3) hot-die pressing, (4) hot-isostatic pressing, (5) powder extrusion (with or without a binder) followed by sintering, (6) forging of powder preforms, (7) activated sintering, (8) liquid phase sintering, and (9) sintering with a pore forming filler material (e.g., wax, bicarbonates, etc.). A few porous structures which were produced by some of the above techniques are illustrated and briefly discussed below. These structures are similar to those required for heat pipes, though they have not been optimized as heat-pipe structures, since they were produced for other applications.

Pressureless sintering was used to produce the porous structures shown in Figure 6. The structure was electron-discharge-machined to the configuration shown, and the solid cap was attached by electron-beam welding; a technique which could be used for heat pipe end closure. Note that the pore shape of the structure is influenced considerably by the powder shape. Spherical powders produce a rounded pore, while irregularly shaped powders produce complex and irregular pore shapes. Figures 7 and 8 illustrate measured pore distribution for these two structures. Note the narrow pore size distribution of these two structures. The width of this distribution can be readily varied by controlling the powder size distribution and the sintering variables. Control of the pore size and distribution will be critical in producing cryogenic heat-pipe wicks. Figure 9 illustrates another structure which is similar to those shown in Figure 6. The porous structures shown in Figure 6 and 9 were produced by pressureless-sintering of a hydropressed powder preform. The preform was produced by hydropressing irregularly shaped powders in an appropriately shaped rubber and metal mold (which defines the part geometry during pressing) thus permitting the fabrication of three-dimensional (other than cylindrical) heat pipe wick structures, particularly for the evaporator and condenser regions.

Still another desirable feature is to be able to produce adjacent sections of a heat pipe with small pores followed by portions with larger pores. Figure 10 illustrates a porous structure fabricated at BCL which contained adjacent small and large pore size regions. The interface of the two regions is well defined and continuity of the structure is preserved across the interface. Thus, a graded wick structure between evaporator, adiabatic and condenser regions can be fabricated.

Figure 11 shows a method for producing controlled porosity tubing which is currently being investigated by BCL. Tubing is extruded from a mixture of binder, moisturizers, and metal powders. The extrusion operation requires low pressures and is suitable for producing tubing up to 20 feet in length (well above most present requirements). After extrusion the binder is removed by oxidation and the tubes are sintered in hydrogen. A cross section of an extruded and sintered copper tube (1/8-in. O.D. x 1/32-in. wall) is shown in Figure 12. Figures 13 and 14 show cross sections of similar tubes which have been produced from Type 316L stainless steel powder and illustrate the porosity control which can be achieved. The cold-binder extrusion method, although not producing the optimum wick for the cryogenic

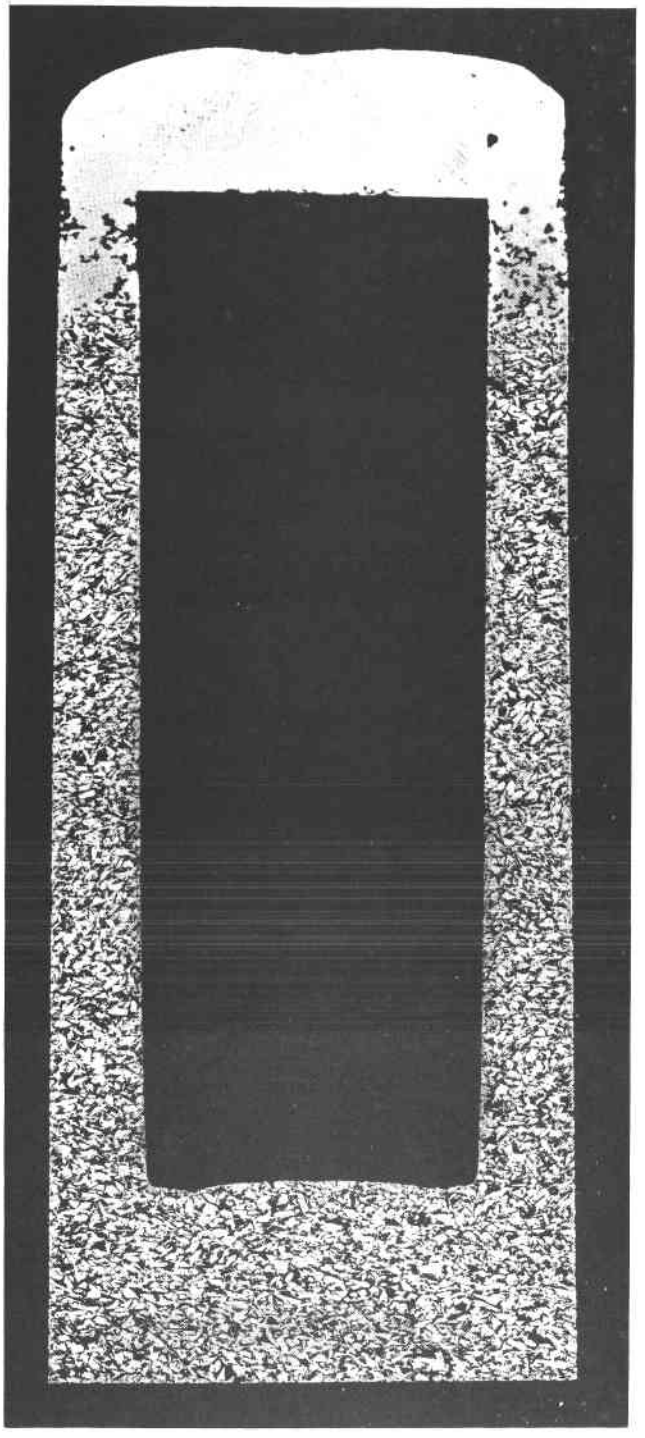

9X 2E757

Irregular Powder Structure

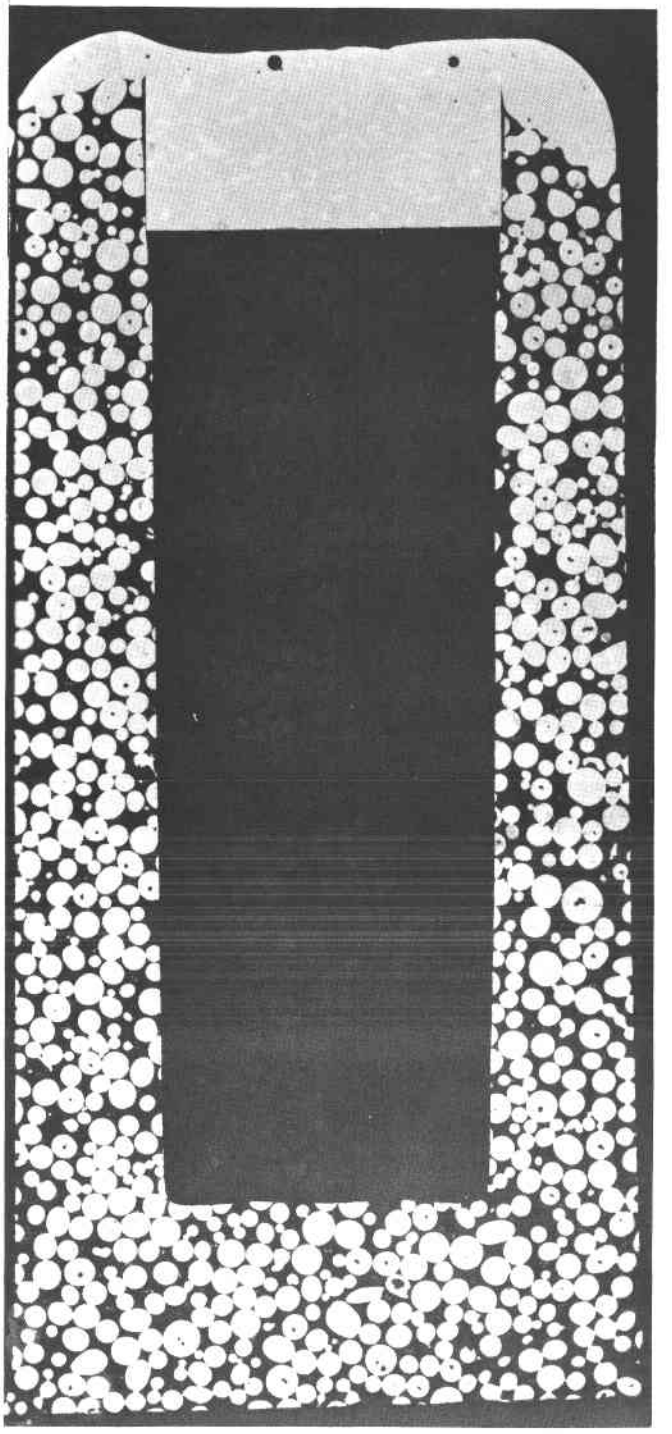

9X 6E201

Spherical Powder Structure

FIGURE 6. PRESSURELESS-SINTERED STRUCTURES PRODUCED FROM IRREGULAR AND SHPERICAL POWDER

Central cavity formed by electrodischarge machining pressureless-sintered porous body and solid cap attached by electron-beam welding.

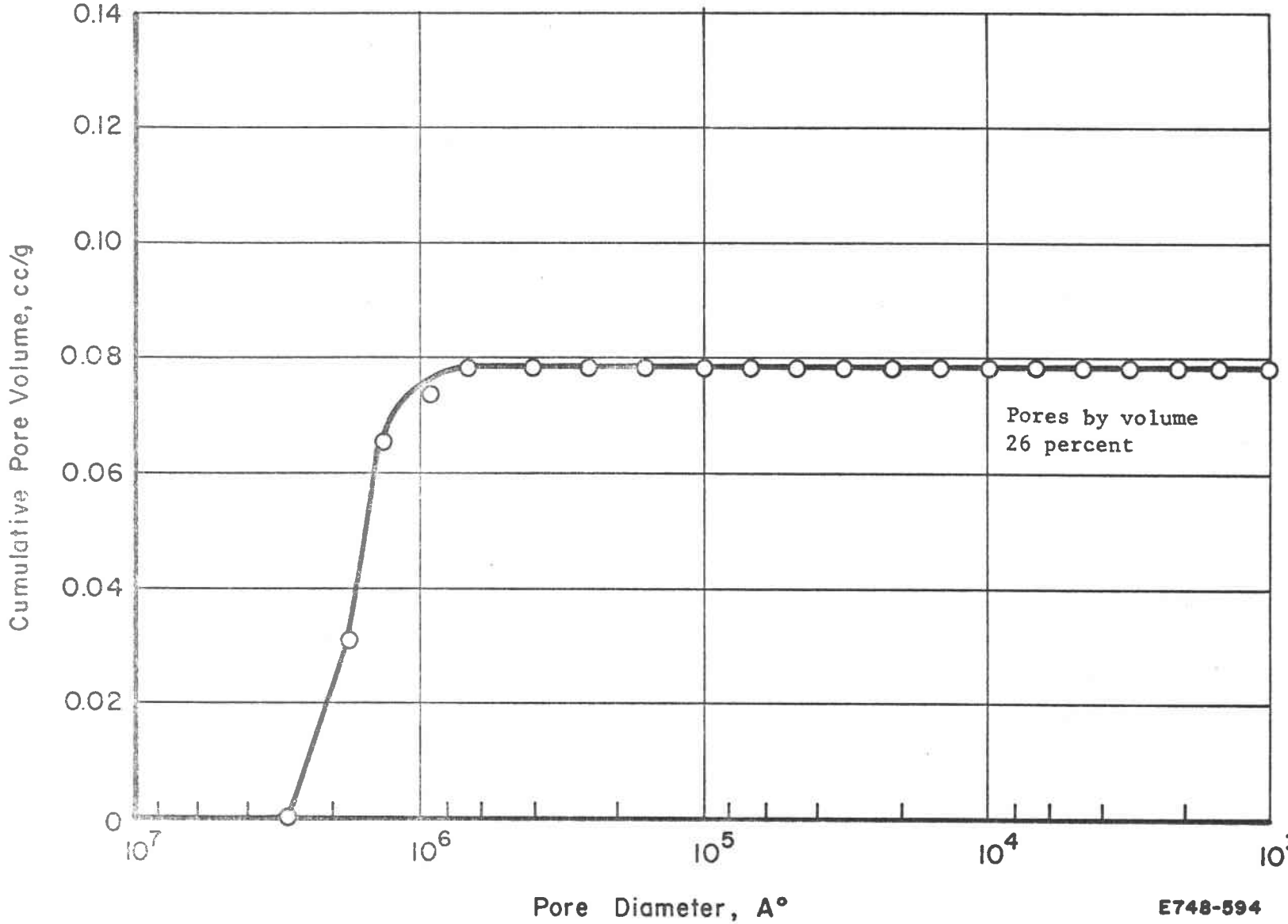

FIGURE 7. PORE SIZE DISTRIBUTION OF PRESSURELESS-SINTERED SPHERICAL POWDER STRUCTURE

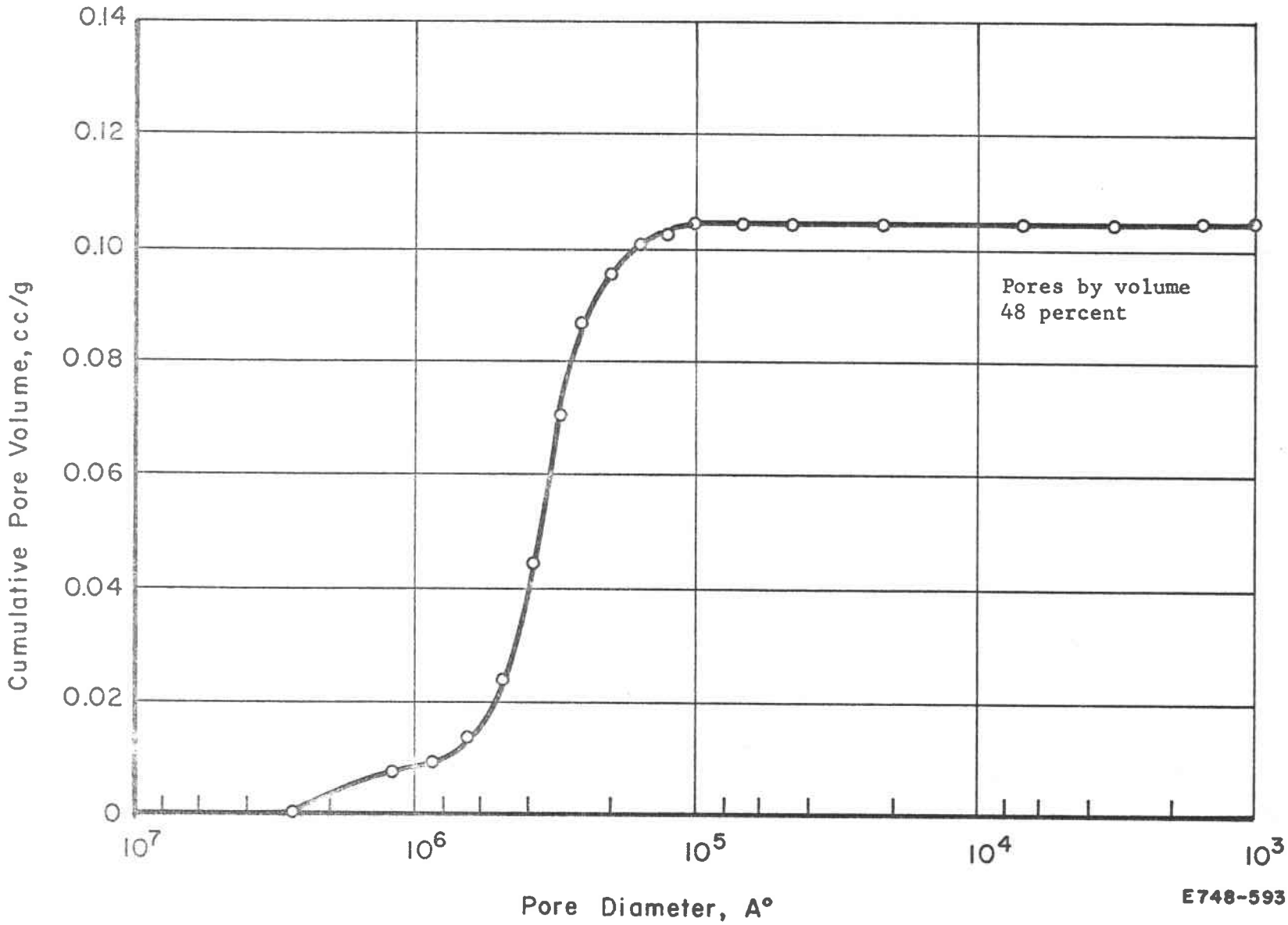

FIGURE 8. PORE SIZE DISTRIBUTION OF PRESSURELESS-SINTERED IRREGULAR POWDER STRUCTURE

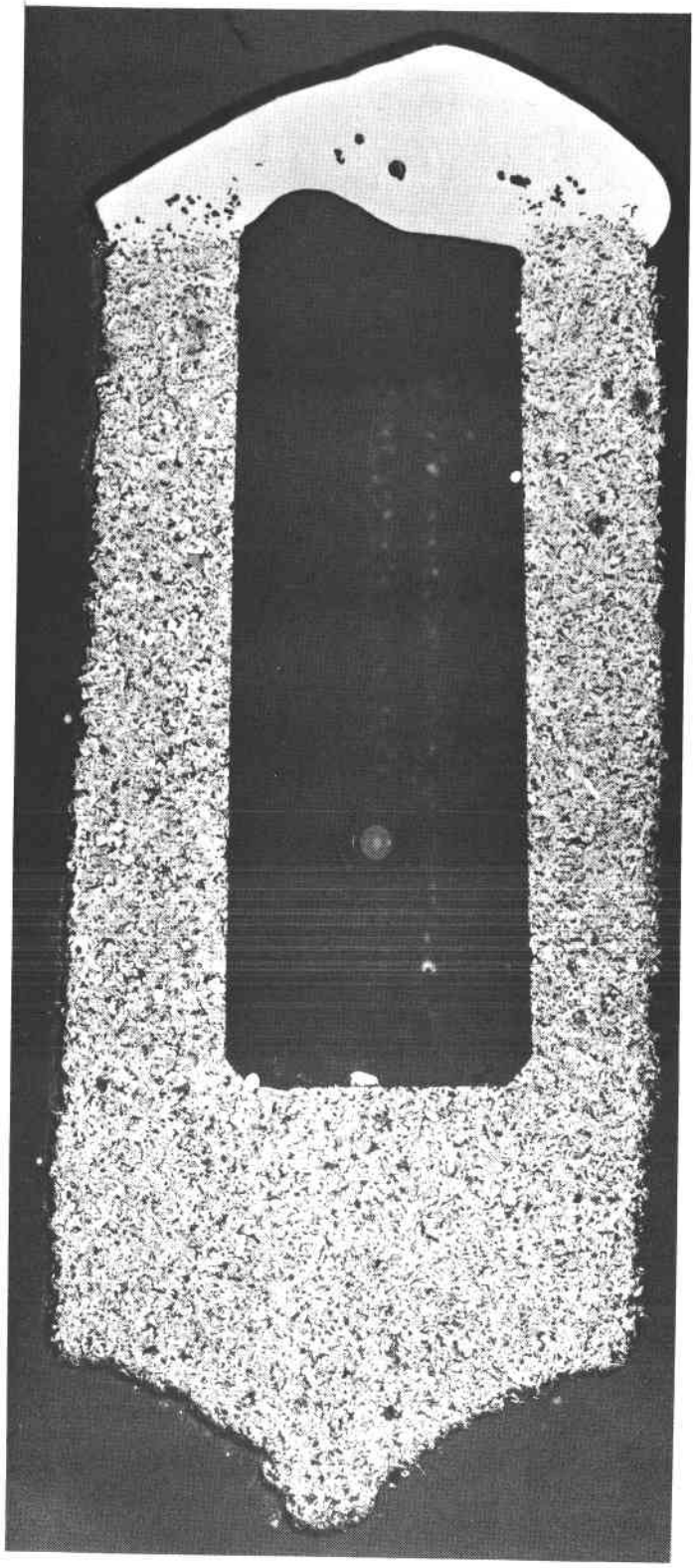

9X DE658

FIGURE 9. A PRESSURELESS-SINTERED COMPONENT PRODUCED FROM A HYDROPRESSED PREFORM OF IRREGULAR POWDERS

Solid cap attached by electron-beam welding.

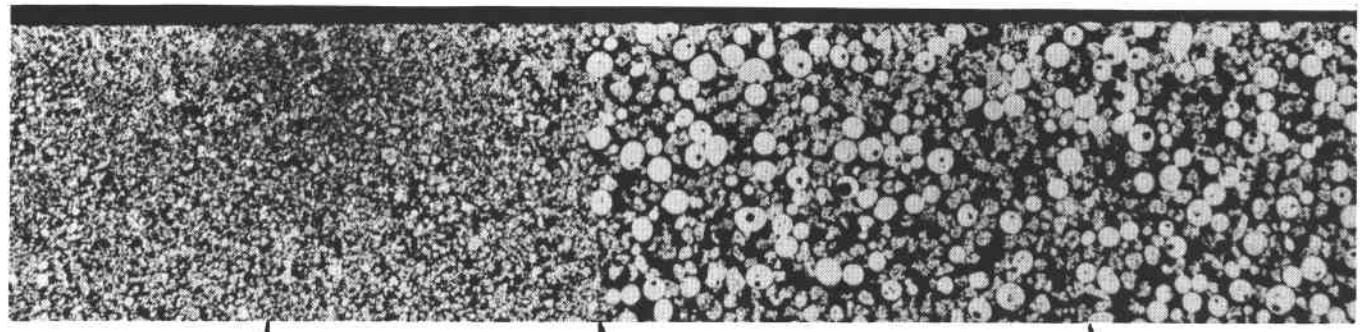

a. Composite of Structure

5E468

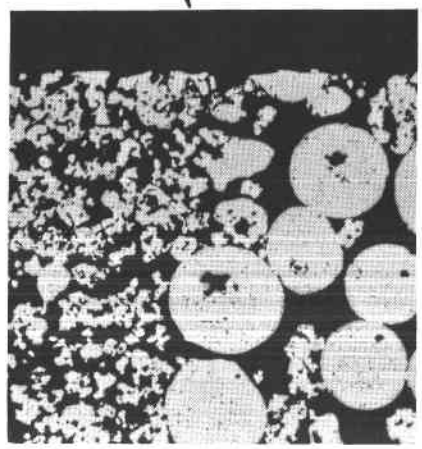

5E411

c. Interface of Small- and Large-Pore-Size Regions

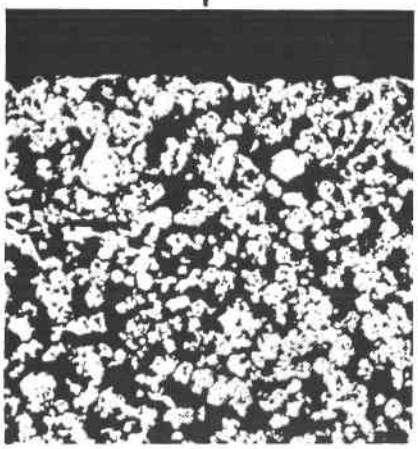

5E412

b. Small-Pore-Size Structure

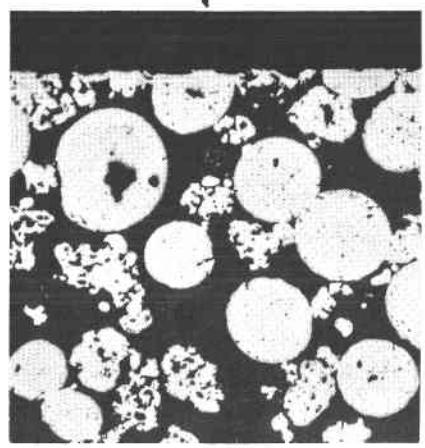

5E410

d. Large-Pore-Size Structure

FIGURE 10. POROUS COPPER STRUCTURE CONSISTING OF SMALL- AND LARGE-PORE-SIZE REGIONS

The structure was produced by pressureless sintering.

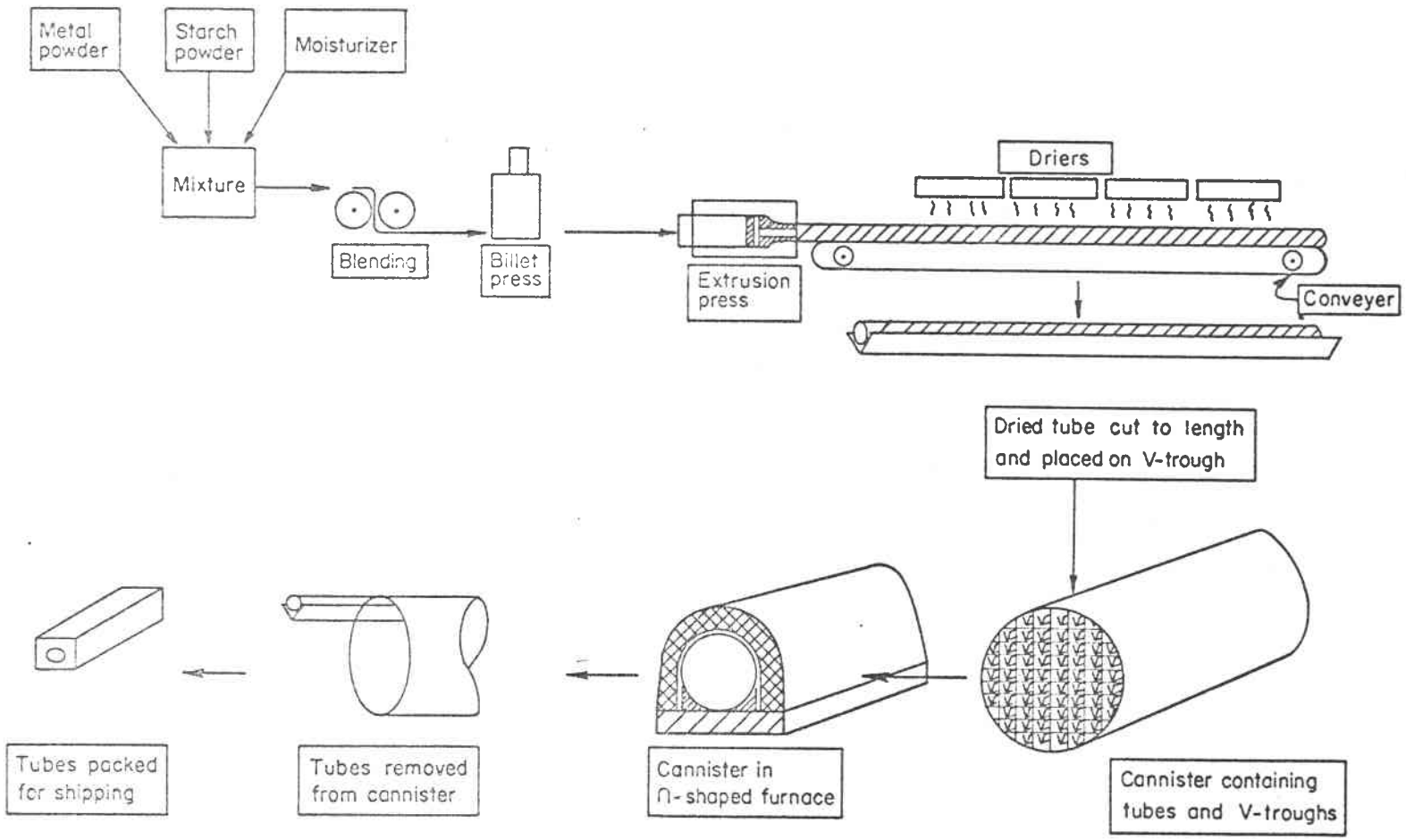

FIGURE 11. FLOW DIAGRAM FOR MASS PRODUCTION OF POROUS TUBES FABRICATED BY COLD-BINDER EXTRUSION FOLLOWED BY SINTERING

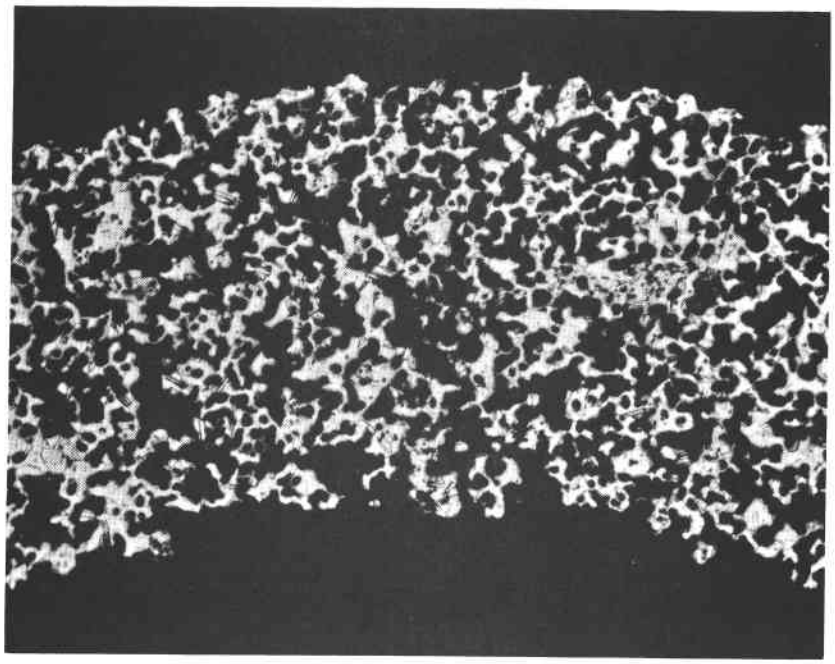

100X 2E513

Fine-Pore-Size Copper Tube

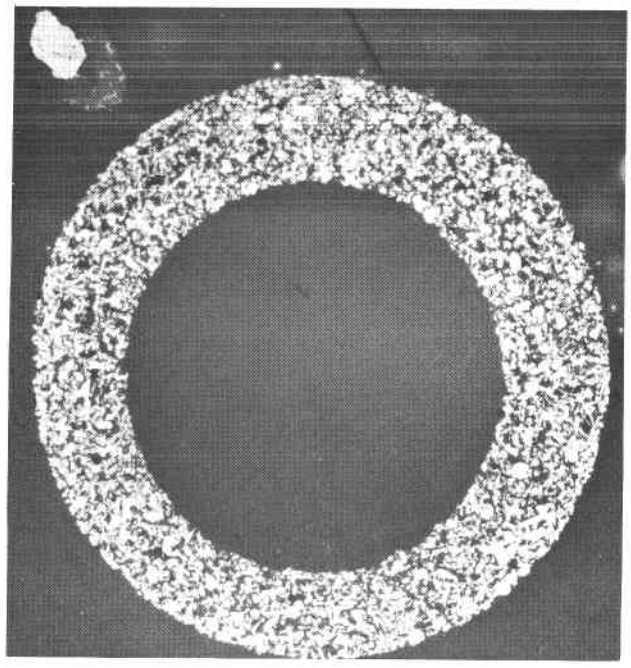

15X 2E591

FIGURE 12. TYPICAL WALL CROSS SECTION OF THE AS-SINTERED COPPER TUBES

The specimens have been polished and etched to reveal the microstructure.

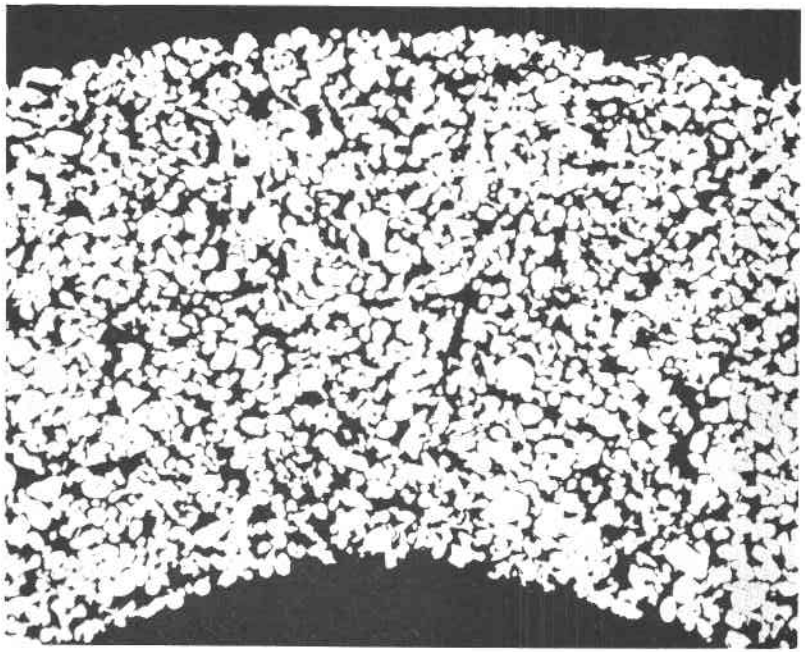

100X 4D902

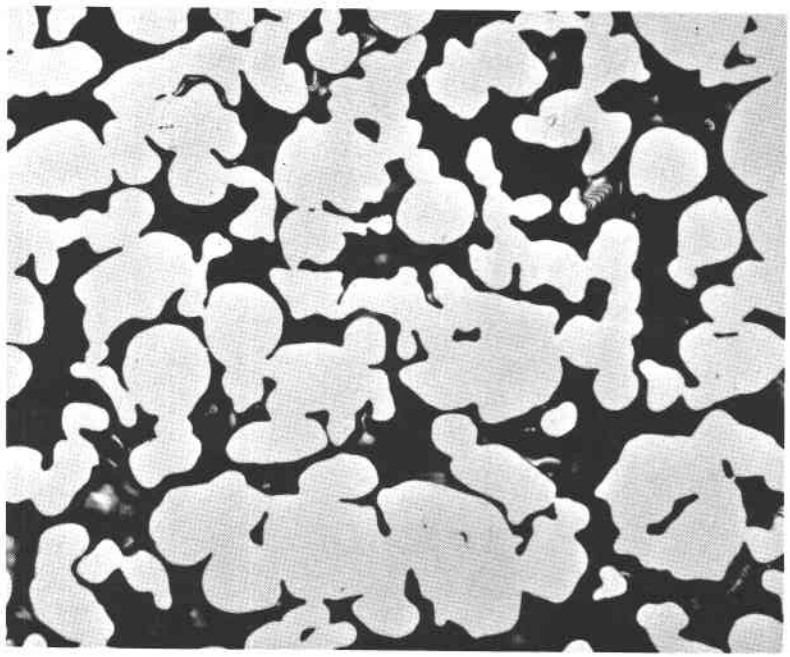

500X 4D906

FIGURE 13. SINTERED S/S 316 POWDER WICK WITH 1-5 μ NOMINAL PORE DIAMETER AND ~20 PERCENT POROSITY (FABRICATED BY PRESSURELESS SINTERING)

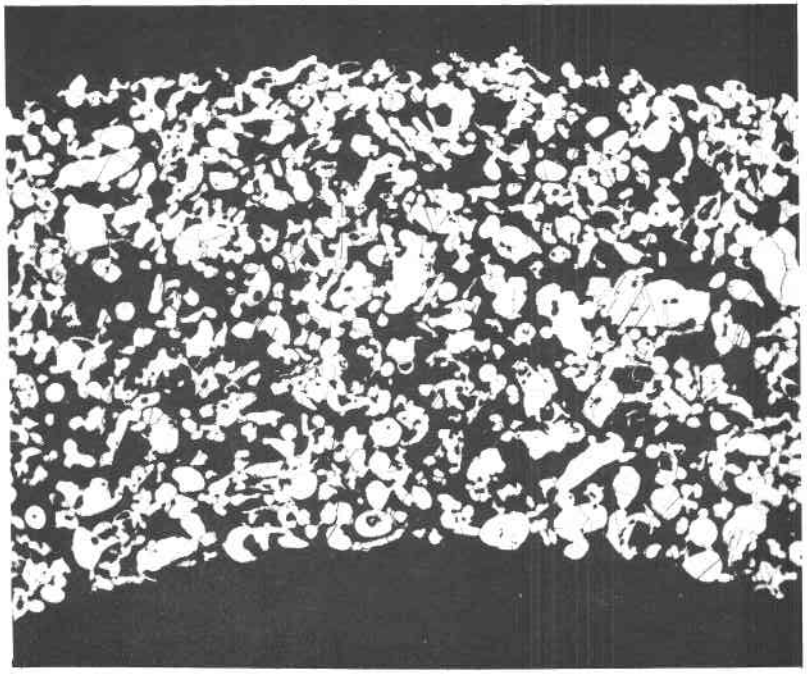

100X 2E506

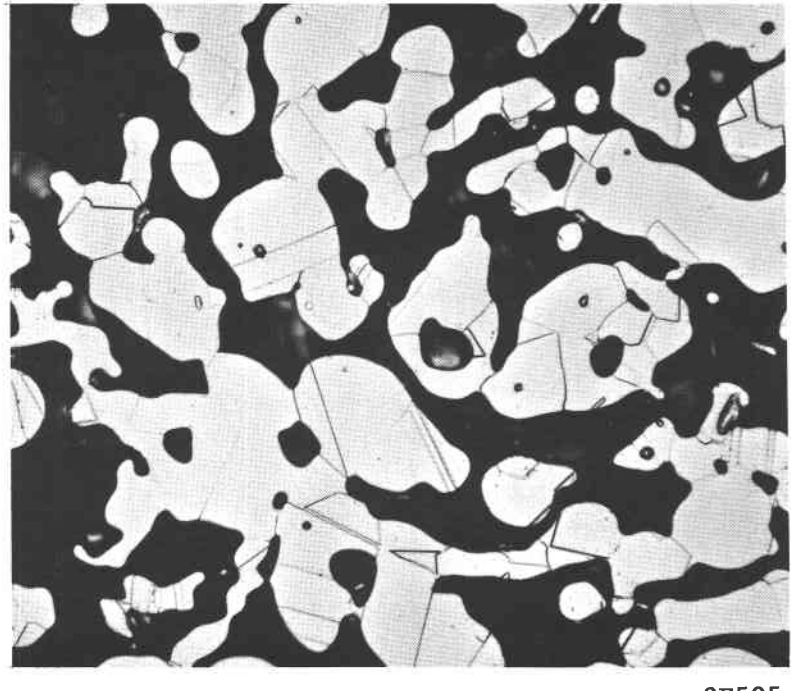

500X 2E505

FIGURE 14. SINTERED S/S 316 POWDER WICK WITH 5-20 μ NOMINAL PORE DIAMETER AND ~44 PERCENT POROSITY (FABRICATED BY PRESSURELESS SINTERING)

heat pipe application, is one of the cheapest, reproducible and most flexible fabrication techniques available. For potential working fluids in the normal ambient range, this method does provide a satisfactory wick structure.

A relatively new wick concept, based on parallel flow channels, has been developed and affords a significant increase in heat pipe performance. The hydrodynamic advantages of the parallel capillary channel (PCC) wick (see Figures 15 and 16) are obvious. However, the fabrication of this type of wick (now in initial development and evaluation stages) is complex. The complex fabrication requirements are on the other hand offset by making available a wick structure which can be fabricated with pore diameters ranging from 10 to 300 microns; and having porosities in the range of 40 to 60 percent. The advantages of (1) low viscous losses associated with the return of the condensed working fluid, (2) high thermal conductivity in the evaporator and condenser regions, hence small radial temperature gradients, and (3) a high degree of reproducibility of wick structures, warrant further development; particularly for cryogenic heat pipes where the traditional "slot" wick is virtually impossible to fabricate for the required effective "pore size". These PCC wick advantages result in an order of magnitude increase in the heat pumping capacity as compared with conventional sintered powder wick structures.

Still another wick concept, referred to as the packed-wire wick, is shown in Figure 17 and utilizes the voids formed between closely packed and sintered parallel wires to achieve the "parallel capillary channel" configuration. The general technique for forming and sintering this type of structure has been reported in the literature*. Although this wick concept is limited to relatively low porosities (5 to 7 percent), it does offer a two-fold improvement in the calculated heat-pumping capacity compared with the more porous 20 to 40 percent sintered powder wicks for heat pipes with high L/D's.

Machining of Porous Wick Structures

Fabrication of the heat pipe may require the machining of the porous wick structure. Porous materials are hard to machine due to their low ductility and strength. Machining by common procedures also closes the pores near the surface due to surface metal deformation (smearing). An acid treatment must follow normal machining in order to open the surface pores, but this is a difficult task. Electron-discharge machining (EDM) is a machining technique which circumvents the surface smearing problem. BCL has used EDM to machine porous materials without closing the porous materials structure (see Figures 18 and 19). Figure 20 illustrates the tapered evaporator region of a PCC structure. The oil used during EDM is removed from the porous structure through ultrasonic cleaning in trichloroethylene followed by an ultrasonic rinse in alcohol. The porous structure is then slowly heated under a vacuum to 1400 F to remove any residued material. Porous structures treated in this manner are free of internal contaminants.

---

* Alexander, B.H., and Balluffi, R.W., "The Mechanism of Sintering of Copper", Acta Metallurgica, 5, 666-677 (1957).

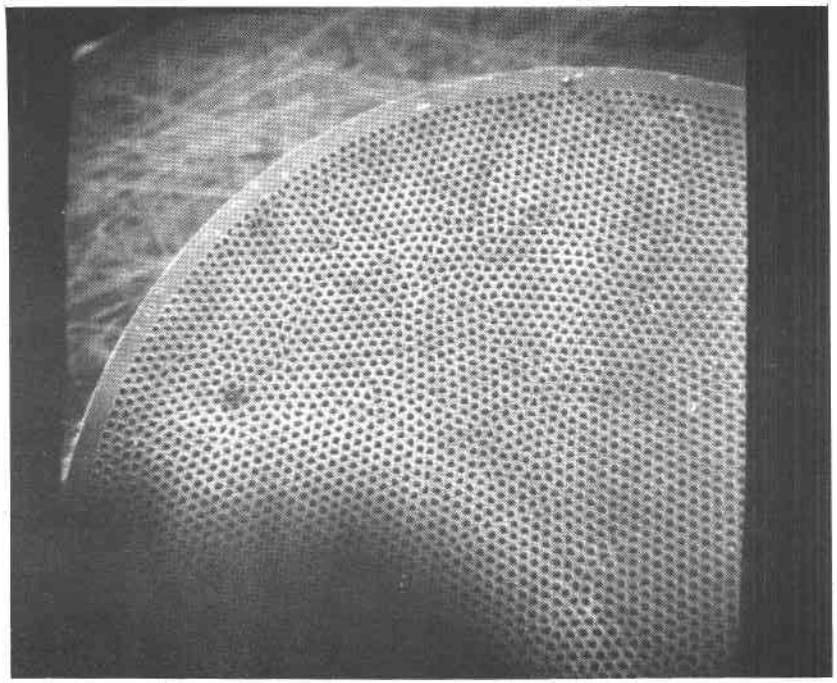

20X

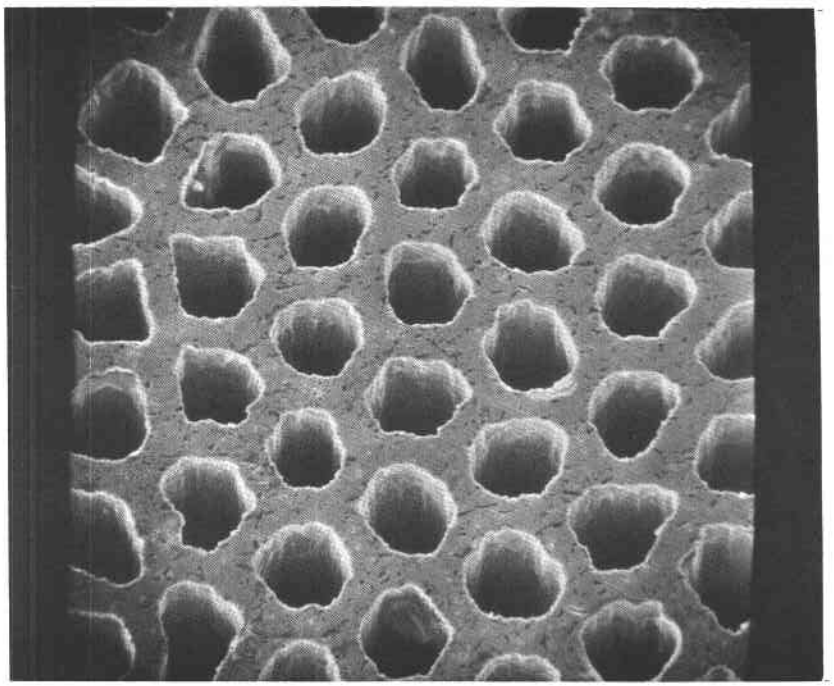

200X

FIGURE 15. S/S 304 PARALLEL CAPILLARY-CHANNEL (PCC) WICK WITH 40 μ NOMINAL PORE DIAMETER AND ~40 PERCENT POROSITY (CENTRAL VAPOR-CHANNEL FORMED USING EDM TECHNIQUES)

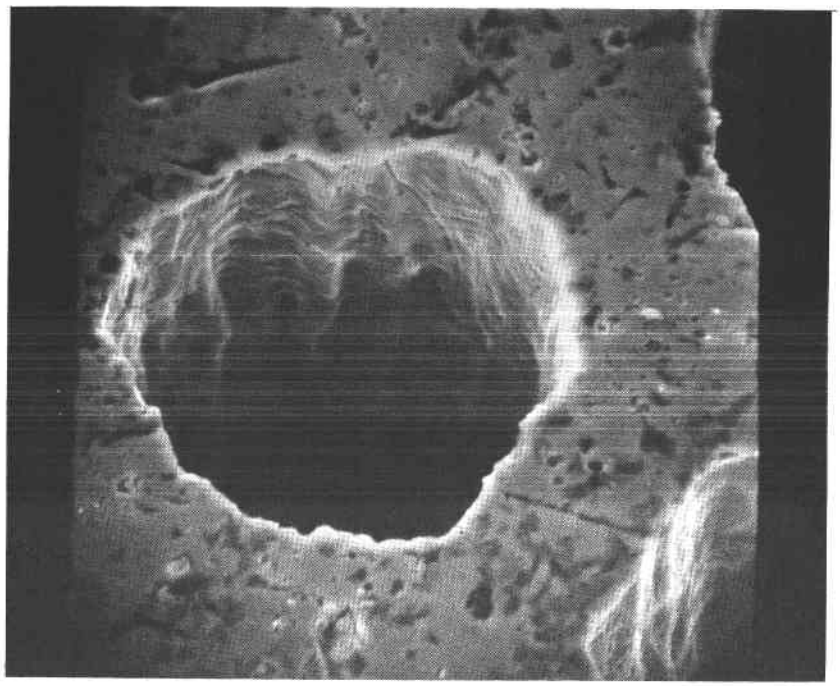

1,000X

FIGURE 16. S/S 304 PARALLEL CAPILLARY-CHANNEL (PCC) WICK WITH 40 μ NOMINAL PORE DIAMETER AND ~40 PERCENT POROSITY

Security is...

Your entry blanks for the "SECURITY IS" Contest are in the back of this pad.

cold-binder extrusion method (botta, p 25
- best for normal ambient range.

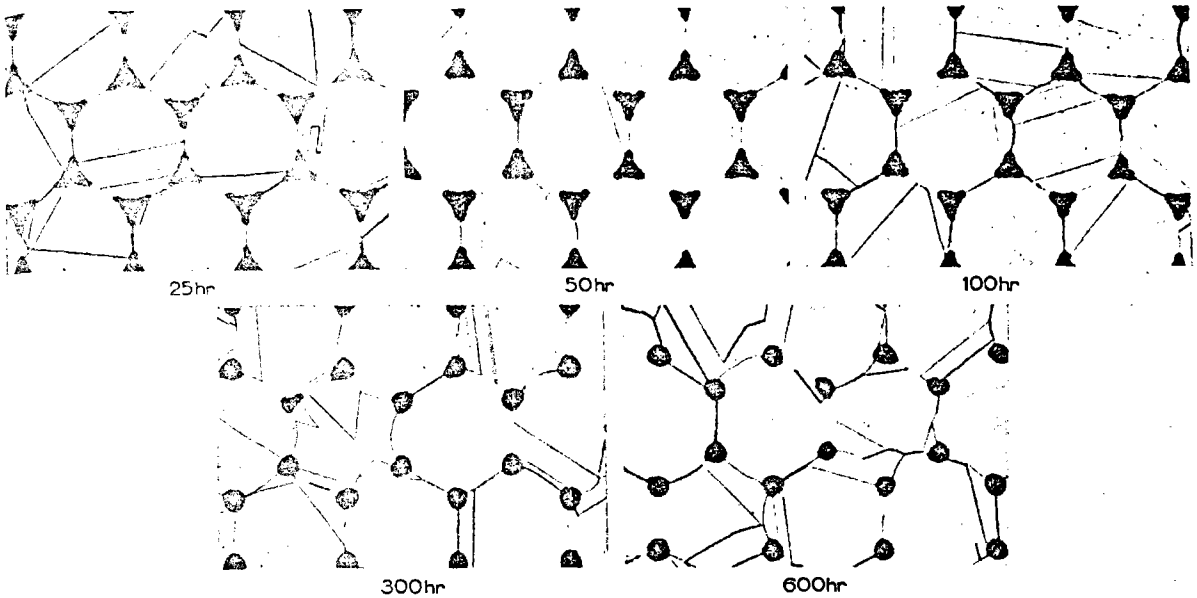

FIGURE 17. CROSS-SECTION OF PACKED-WIRE WICK AFTER SINTERING AT 900 C [See Reference (1)]

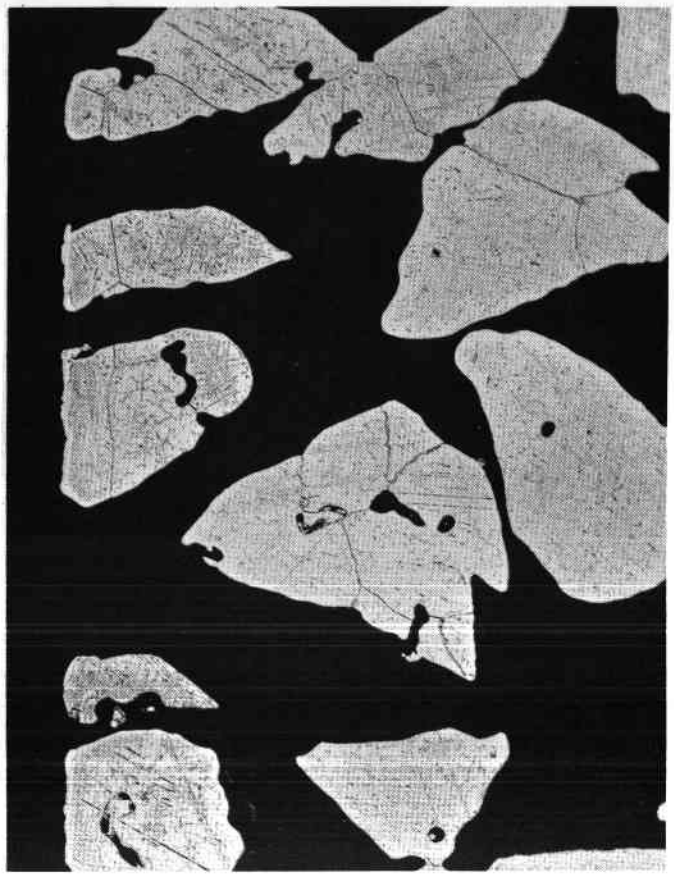

500X 2E307

FIGURE 18. SINTERED STELLITE-21 POWDER WICK WITH 25 μ NOMINAL PORE DIAMETER AND ~46 PERCENT POROSITY (NOTE THE DESIRABLE PORE EXPOSURE ACHIEVED AT THE LEFT EDGE USING ELECTRODISCHARGE MACHINING TECHNIQUES)

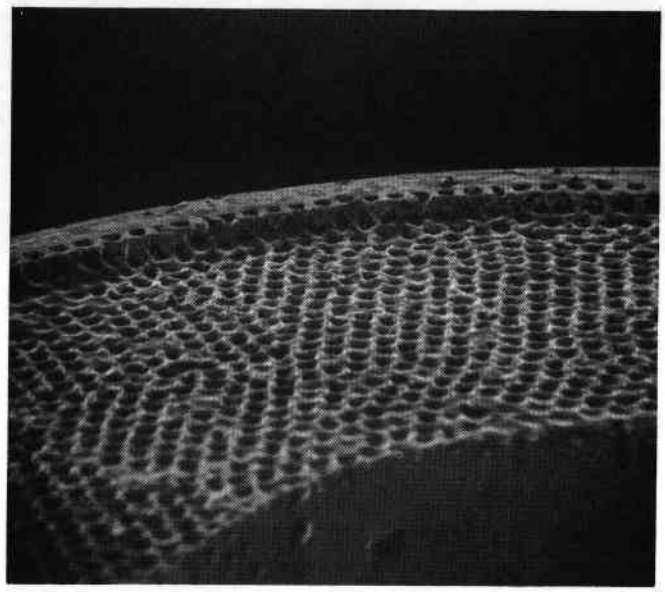

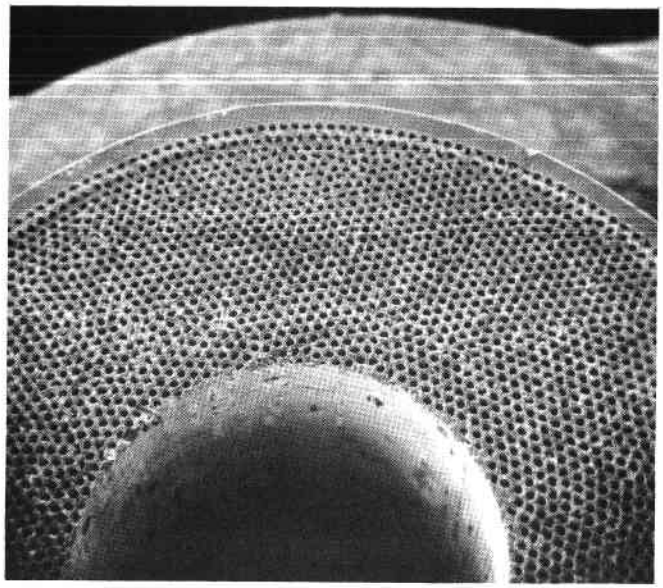

FIGURE 19. CAPILLARY CHANNEL WICK SHOWING EDM COUNTERBORE AS MACHINED

Note the open pore structure which remans after EDM.

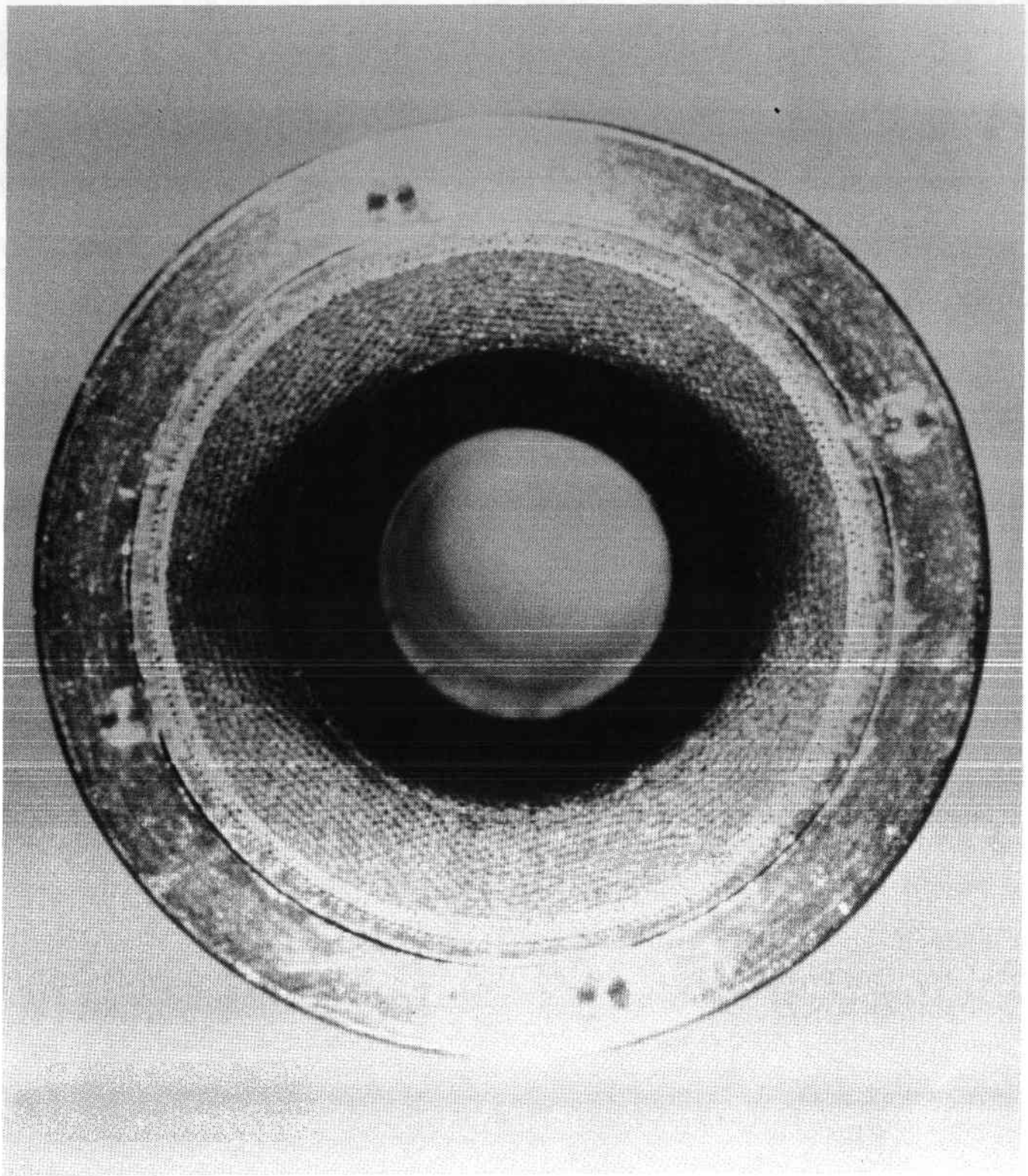

FIGURE 20. TAPERED EVAPORATOR REGION FOR A PCC WICK STRUCTURE

Plating of Porous Structures

The porous wick structure of heat pipes must be sealed in a leak-tight outer envelope (tube) which maintains intimate contact with the wick structure and serves as a pressure container. The evaporator and condenser sections are critical regions which call for metallurgical bonds to reduce thermal impedances. One method of obtaining this leak-tight outer jacket and optimum heat transfer coupling is to deposit a metal on the outer surface of the porous wick. BCL has through relatable programs conducted experiments to prove the potential of obtaining leak-tight metal coating of wicks. Figure 21 shows two porous tubes (Cu-10Ni and copper tubes) which were plated with electroless nickel followed by electroplated nickel (note the two distinct layers of nickel). The electroless plating closed the surface pores due to its voluminous nature and did not significantly close the internal pores. Electroplating followed the electroless plating because the rate of deposition obtained with electroplating is significantly higher than with electroless deposition. The nickel plated porous tubing is leak-tight and will contain pressures commensurate with the thickness of the plating.

Heat Pipe Closure/Seal Techniques

Fabrication of heat pipes through other than powder metallurgical methods would probably require the use of diffusion bonding, brazing, or silver soldering of wick components. BCL has extensive facilities for and considerable experience in these joining methods. Silver soldering and brazing are common joining techniques and require little explanation; but due to wick contamination and/or pore closure cannot be recommended for wick structures having very small pore sizes. Another metallic bonding technique, namely diffusion bonding appears much more attractive. Although diffusion bonding is a relatively new process, BCL has bonded many structures containing intricate channels such as those shown in Figure 22; these structures have been devised for aerospace applications. Bonding is achieved at temperatures which promote interfacial diffusion and the applied pressure insures intimate bond line contact while not deforming the channels of the components. Figure 23 shows the microstructure of a typical diffusion bonded component. Note the uniform microstructure in the bonded region and the lack of a bond interface. Proper bonding procedures result in bond strengths which have very nearly the strength of the base metal.

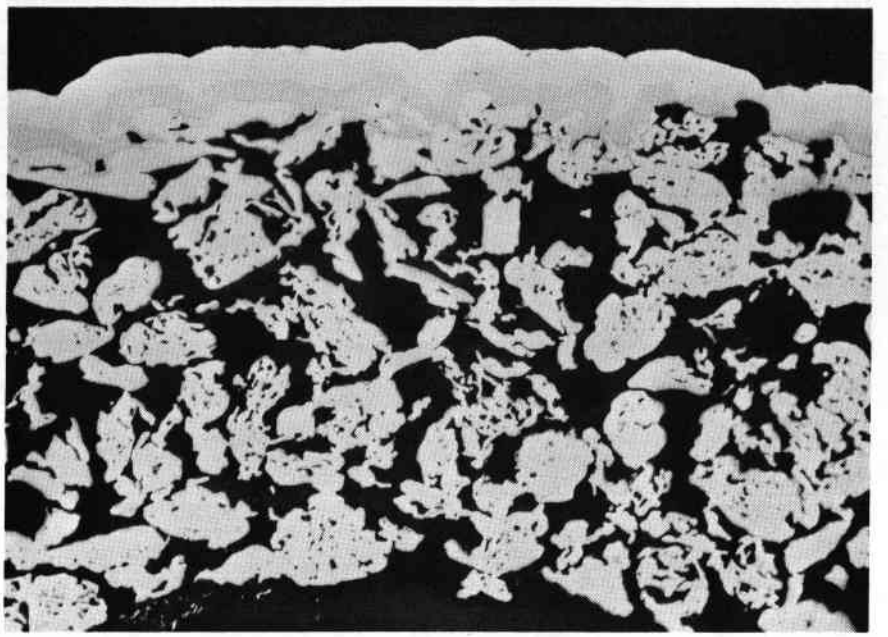

100X 5E409

a. Nickel-Plated Porous Cu-10N Tube

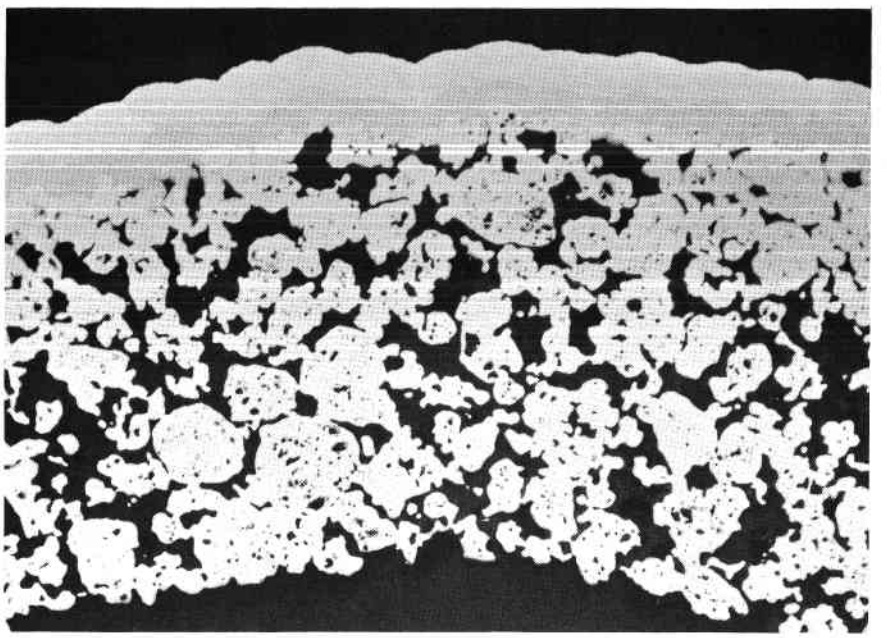

100X 5E407

b. Nickel-Plated Porous Copper Tube

FIGURE 21. NICKEL-PLATED WICK STRUCTURES OBTAINED BY ELECTROLESS PLATING FOLLOWED BY ELECTROPLATING OF NICKEL

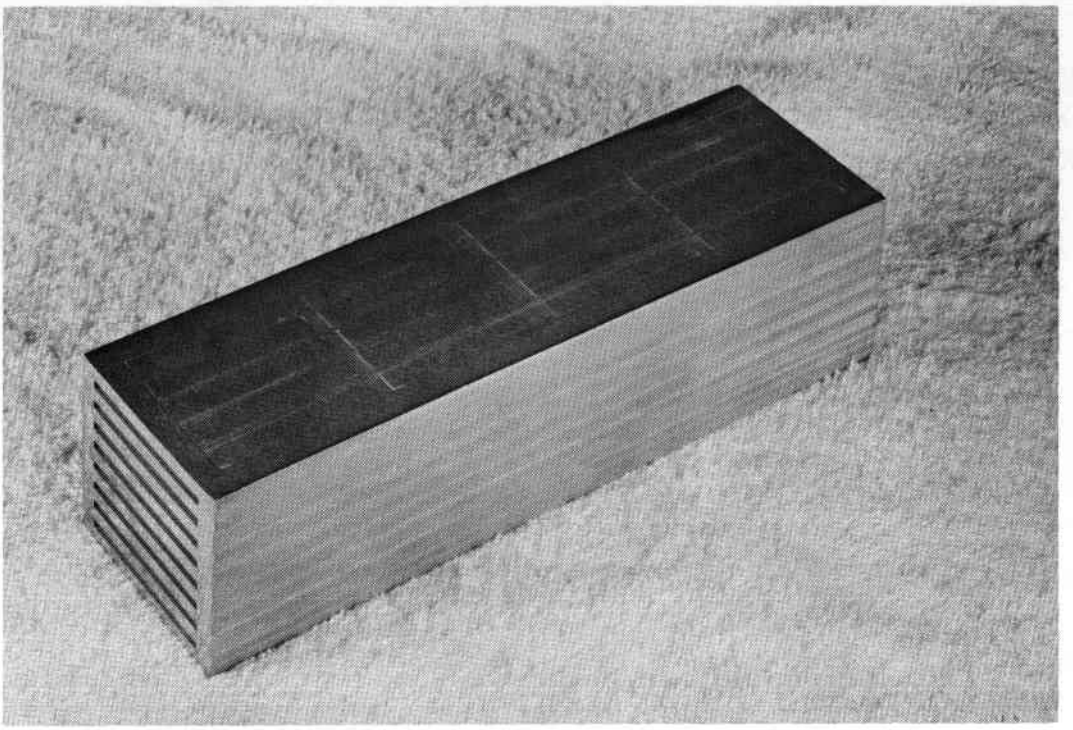

N65596

a. Stainless Steel Diffusion-Bonded Structure

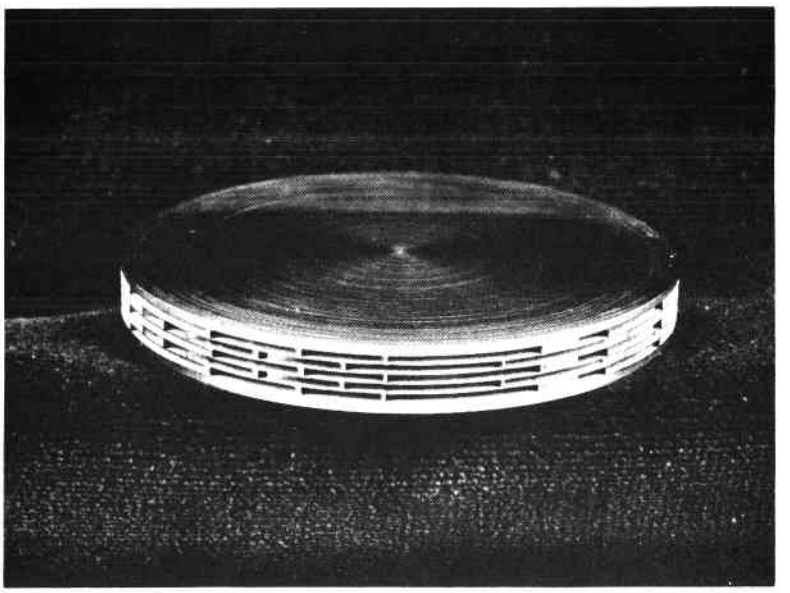

26239

b. Hastelloy C Diffusion-Bonded Structure

FIGURE 22. DIFFUSION-BONDED CHANNEL STRUCTURES

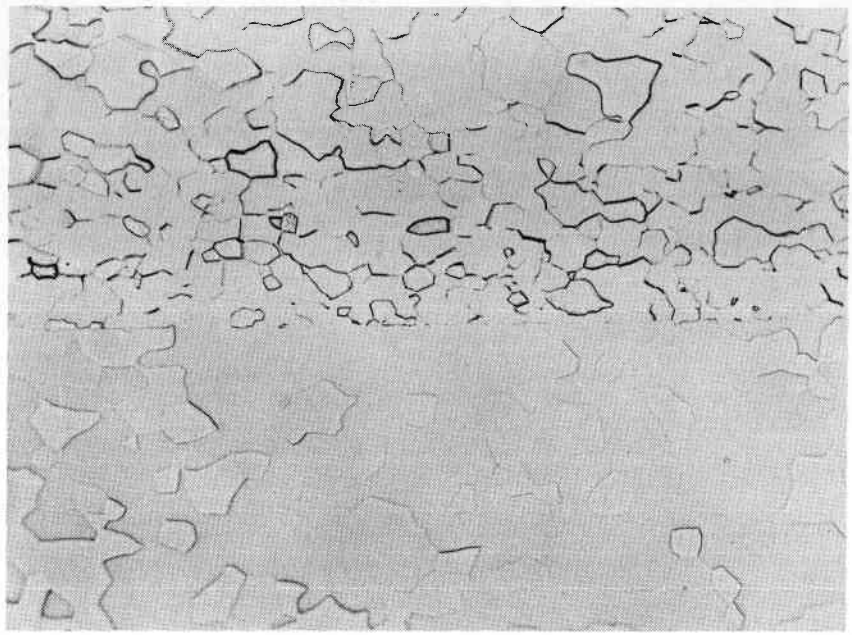

250X N13816

a. As Bonded, 3 Hr, 3000 F, 20,000 Psi

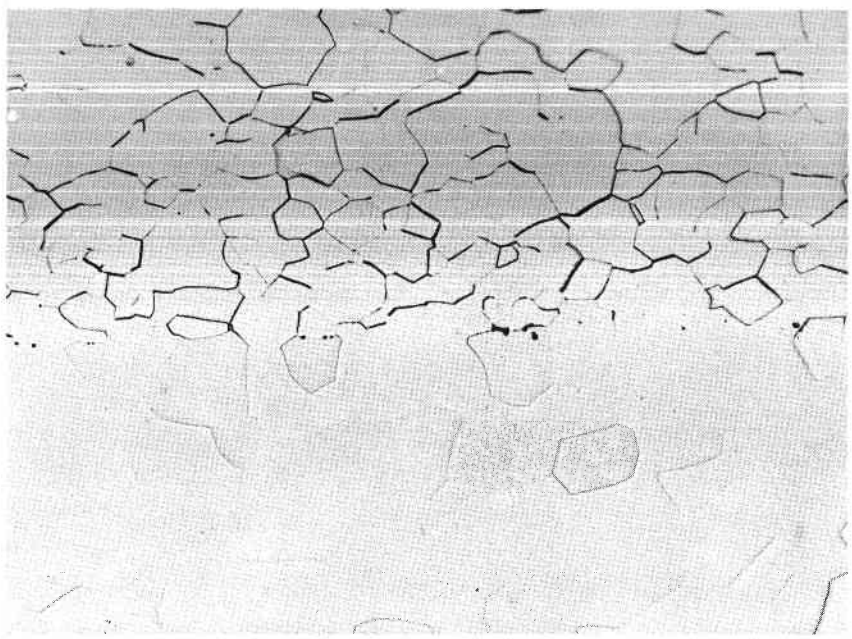

250X N13819

b. Same After Vacuum Heat Treatment, 1 Hr, 4040 F

FIGURE 23. MICROSTRUCTURE OF A TYPICAL DIFFUSION-BONDED COMPONENT OF W AND W-26Re ALLOY

HEAT-PIPE EVALUATION FACILITY

HEAT PIPE LABORATORY

A portion of the BCL heat pipe evaluation facility is shown in Figure 24. Calibrated, distillation type fill apparatus is available for controlled filling procedures. In addition, the heat pipes can be tested in a variety of attitudes. Testing is carried out in an evacuated quartz tube mounted on the rotatable table (see Figure 24) to negate convection effects. The experimental facilities are designed to permit the testing of small-scale heat pipe assemblies such as shown in Figure 25, without resorting to final, "absolute" closure (an interference fit is employed followed by soldered or brazed sealing operation) thus permitting both component, or subassembly, evaluations to be carried out. The same experimental apparatus can then be used to evaluate closed pipe assemblies. A typical experimental assembly prior to insertion into the quartz tube is shown in Figure 26.

Presently available equipment is designed for the following range of operations:

Heat-pipe diameters:	.062 to 1.0-in. diameter
Heat-pipe lengths:	Up to 36 inches
Operating temperatures:	-330 F to 900 F
Heat-pumping capability:	Up to 200 watts
Inclination attitudes:	ϕ_z = 0 to 360 degrees

Expansion, or extension, of the performance evaluation facilities is relatively straightforward and simple. Available, peripheral data readout equipment and electronics are employed. Temperatures and distributions of the heat pipe surface are obtained by means of an infrared scanner. The scanner is mounted on the turntable (see Figure 24) below the quartz tube. Figure 27 illustrates performance data which are typical of the type of correlation achievable in the BCL heat pipe evaluation laboratory.

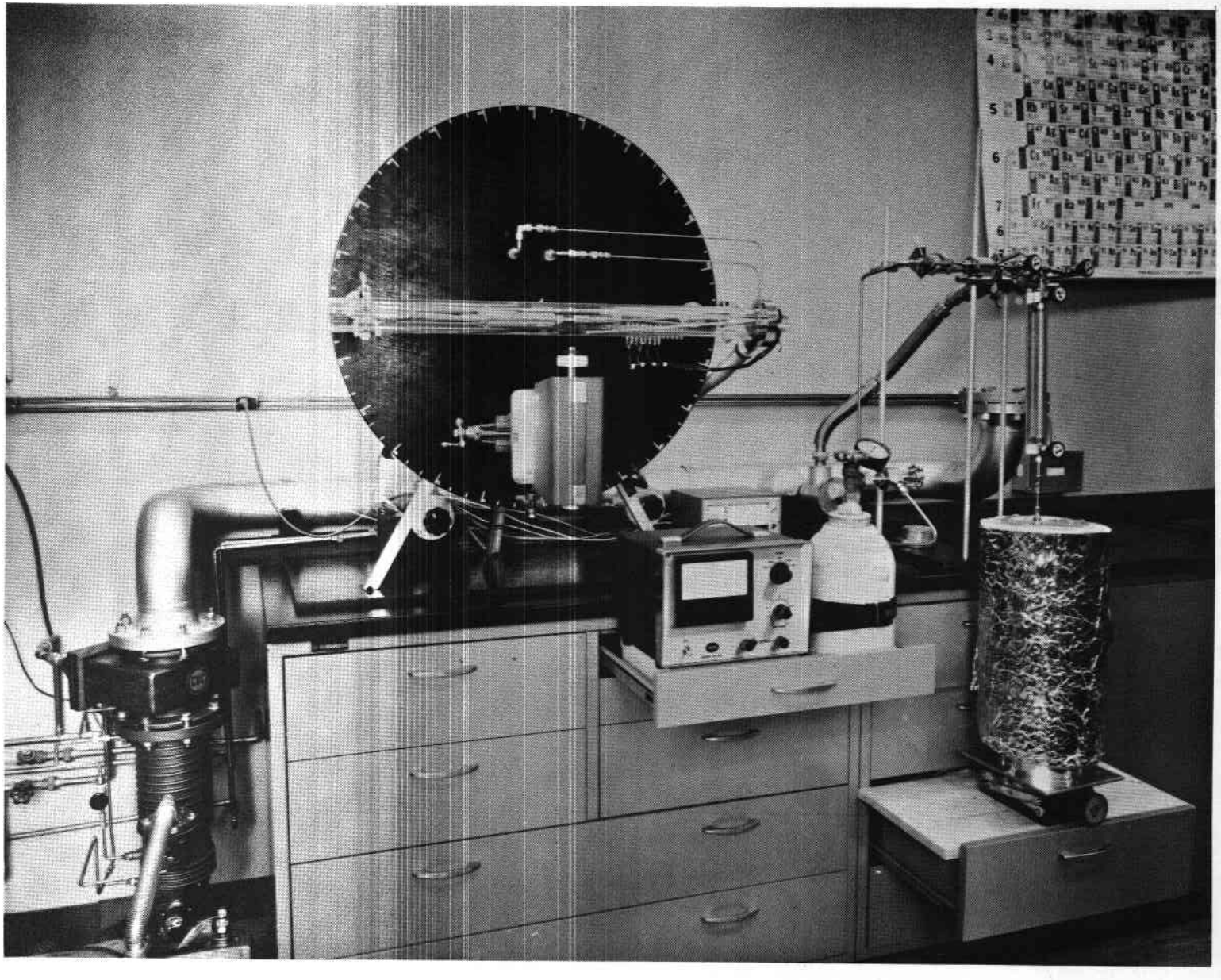

FIGURE 24. HEAT-PIPE EVALUATION FACILITY (HEAT-PIPE TEST APPARATUS ON ROTATABLE PLATFORM ON LEFT AND DISTILLATION-TYPE CHARGING APPARATUS ON RIGHT)

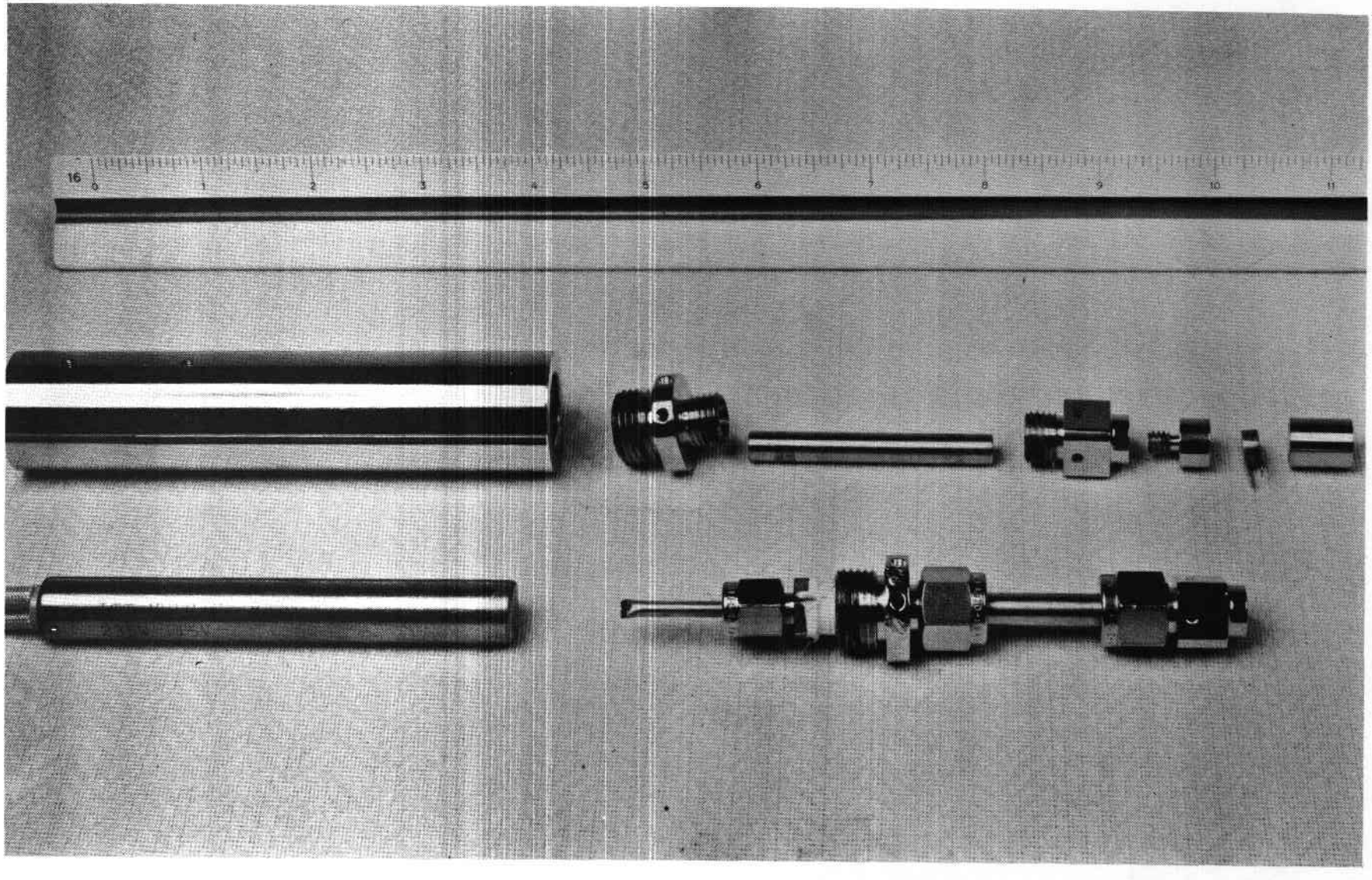

FIGURE 25. DETAIL OF HEAT-PIPE EVALUATION APPARATUS SHOWING CARTRIDGE HEATER, HEAT SOURCE, CHARGING TUBE AND ASSEMBLY, HEAT PIPE WITH SWAGELOK SEALS, AND HEAT-FLUX TRANSDUCER

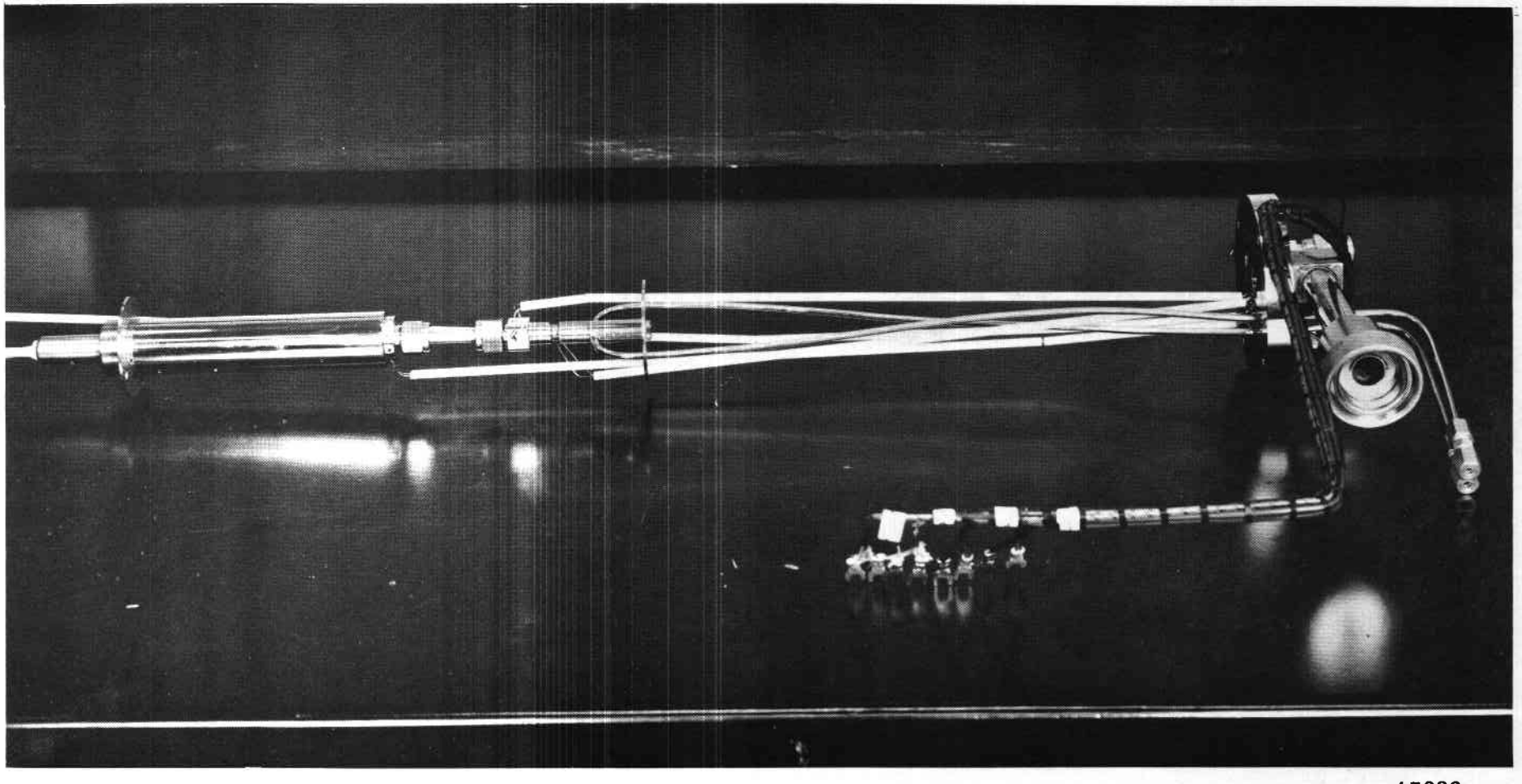

47980

FIGURE 26. HEAT-PIPE EVALUATION APPARATUS

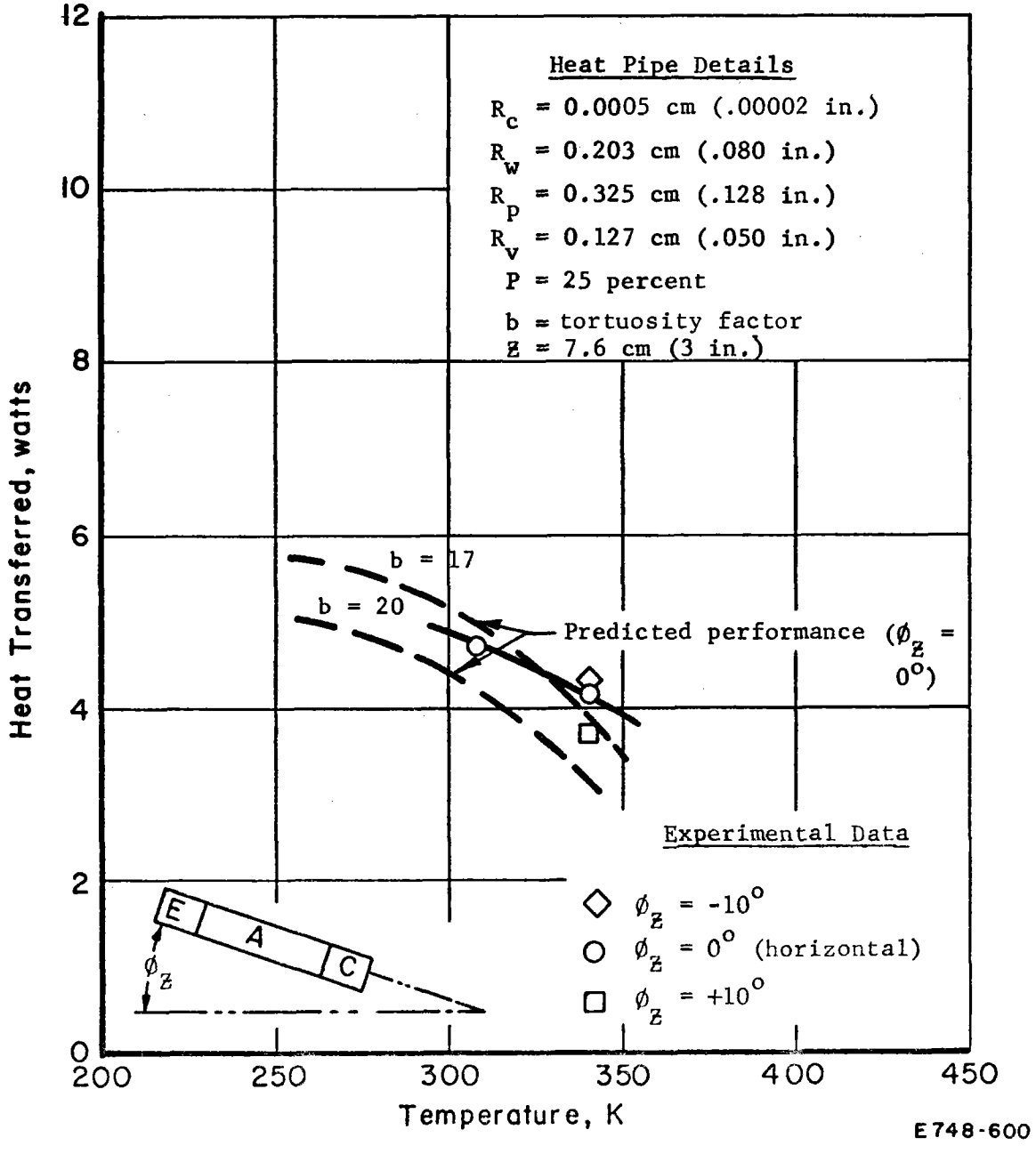

FIGURE 27. COMPARISON OF THEORY WITH EXPERIMENT, FREON HEAT PIPE WITH SINTERED POWDER WICK

SAMPLE HEAT-PIPE DESIGNS AND EXPERIMENTAL RESULTS

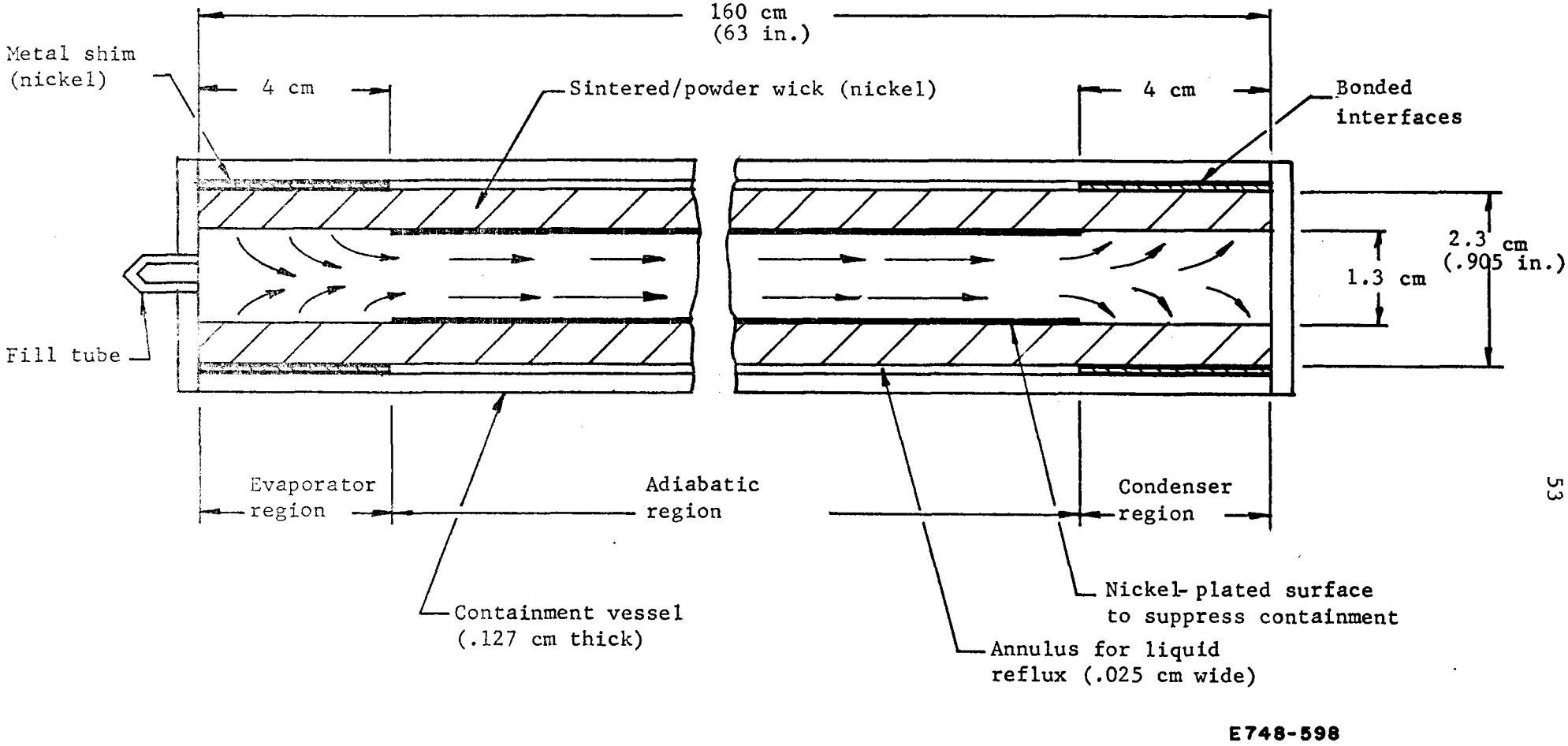

FIGURE 28. SAMPLE HEAT PIPE DESIGN INVOLVING SINTERED POWDER WICK WITH ANNULUS

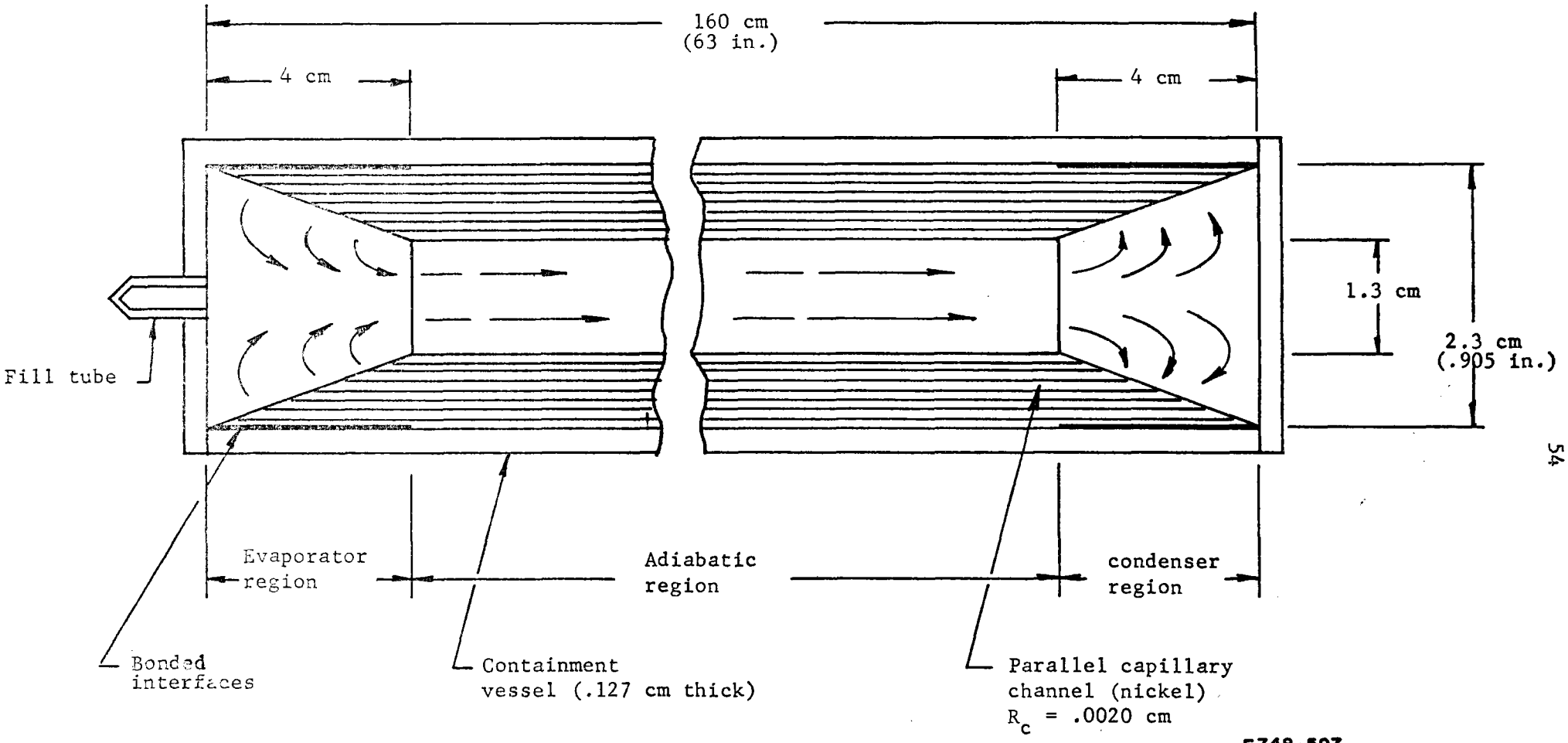

FIGURE 29. SAMPLE HEAT PIPE DESIGN INVOLVING PARALLEL CAPILLARY CHANNEL WICK

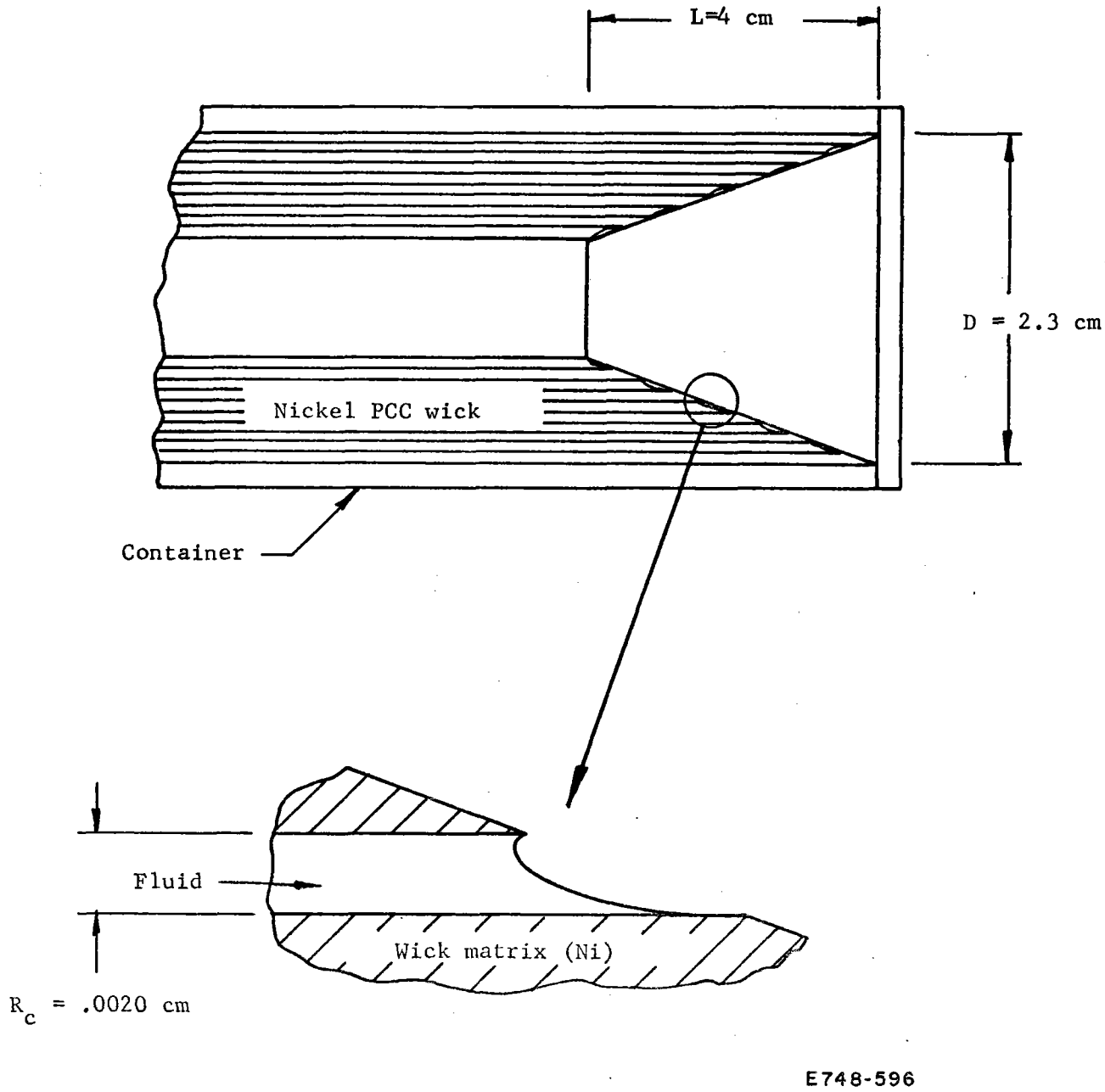

FIGURE 30. PARALLEL CAPILLARY CHANNEL WICK DETAIL FOR ΔT_{fluid} CALCULATIONS

Note: Number of capillary openings in evaporator or condenser (4 cm) $\tilde{=}$ 49,500.

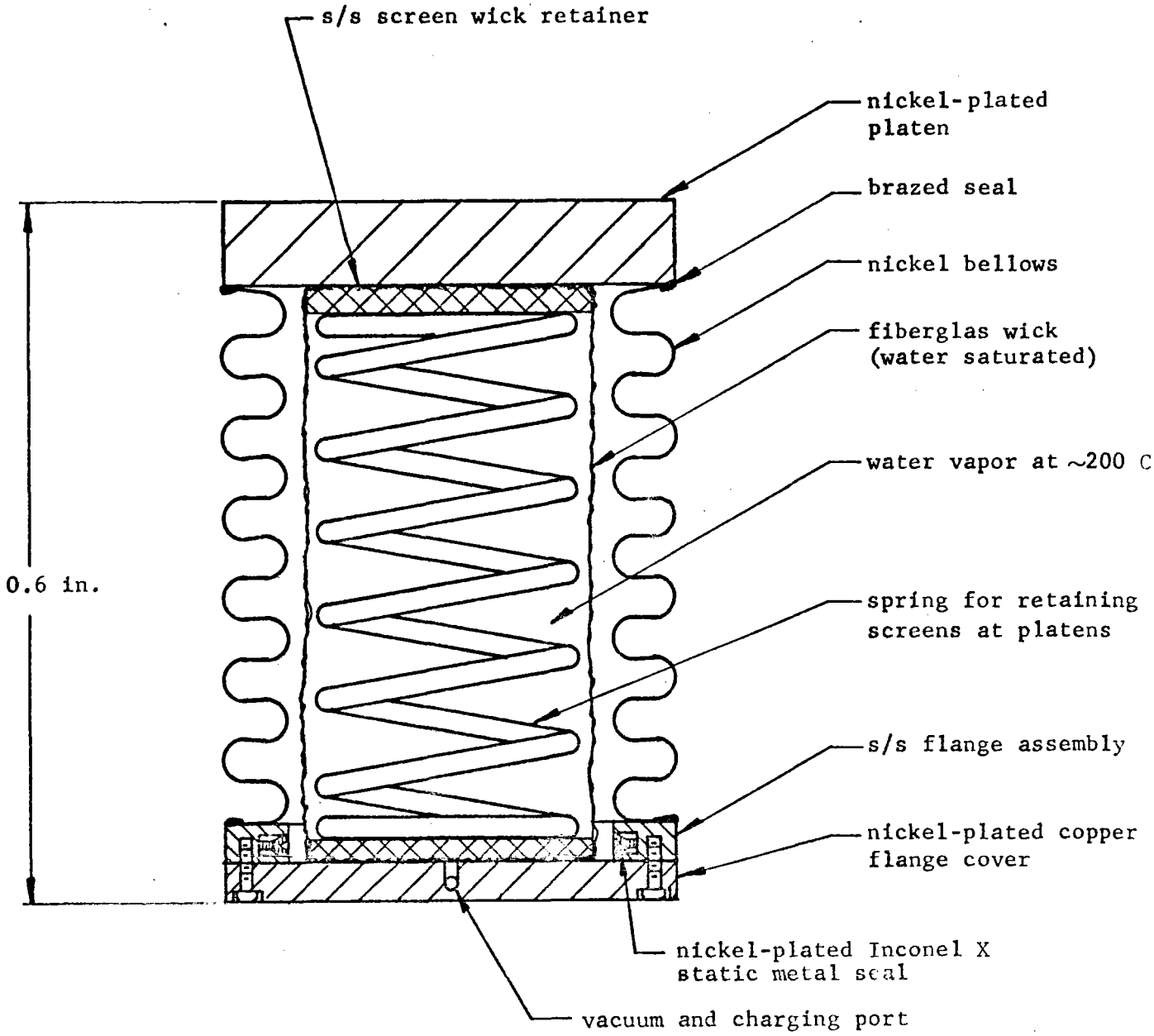

FIGURE 31. BELLOWS HEAT PIPE

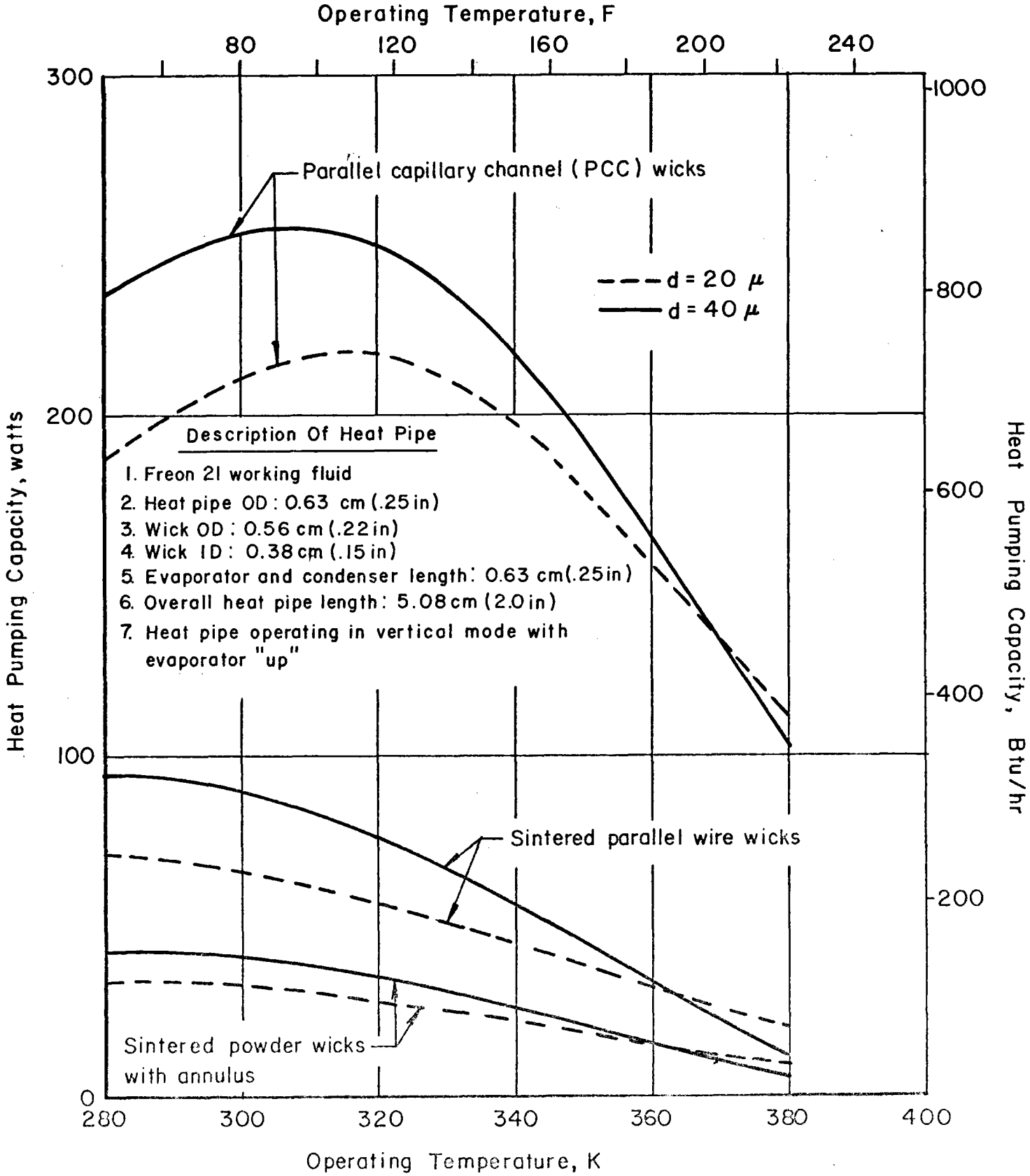

FIGURE 32. COMPARISON OF PREDICTED PERFORMANCE FOR VARIOUS WICK DESIGNS FOR LOW-TEMPERATURE APPLICATIONS

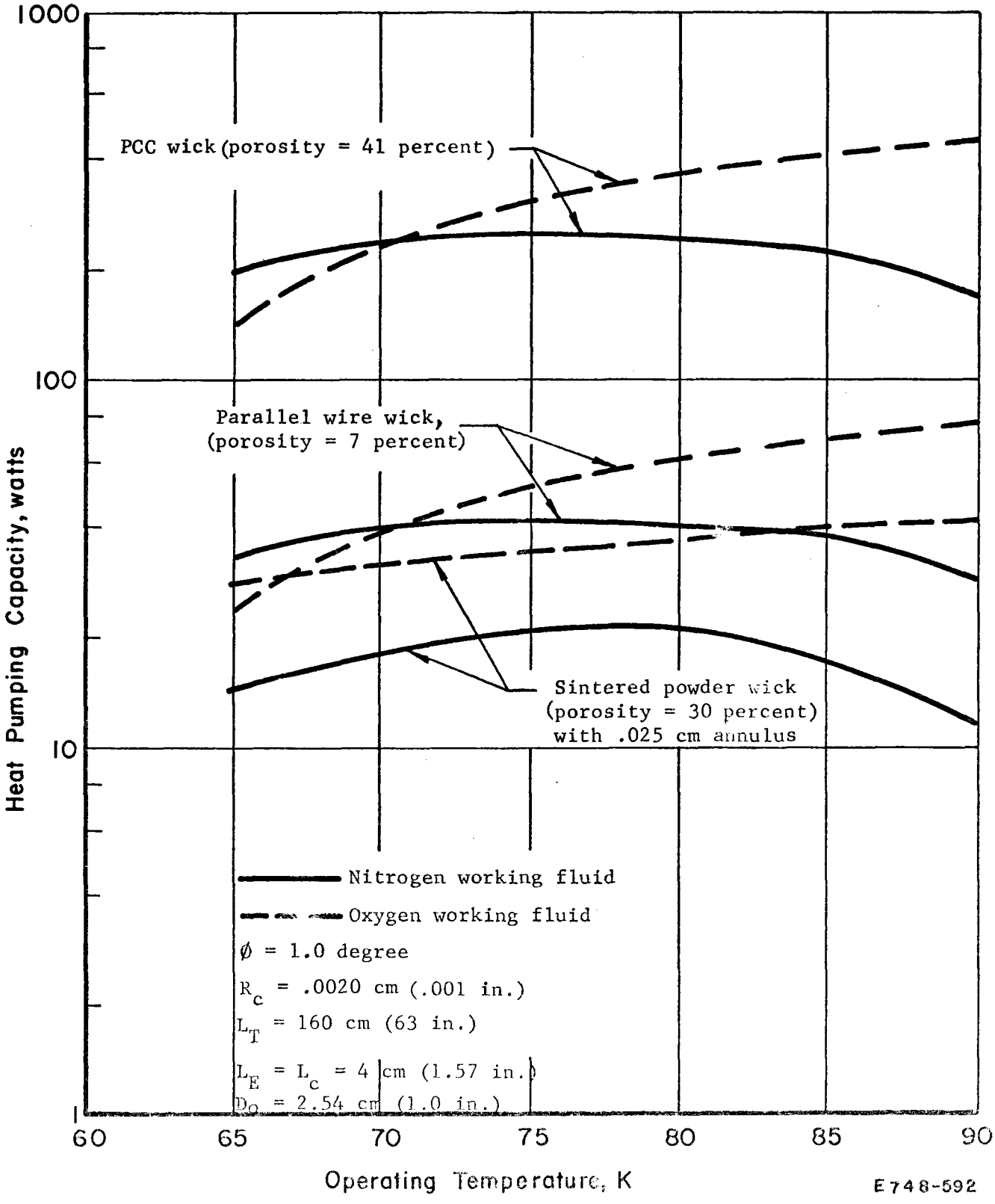

FIGURE 33. COMPARISON OF PREDICTED PERFORMANCE FOR SELECTED WICK DESIGNS SUITABLE FOR CRYOGENIC APPLICATIONS (ϕ_z = 1.0 degree)

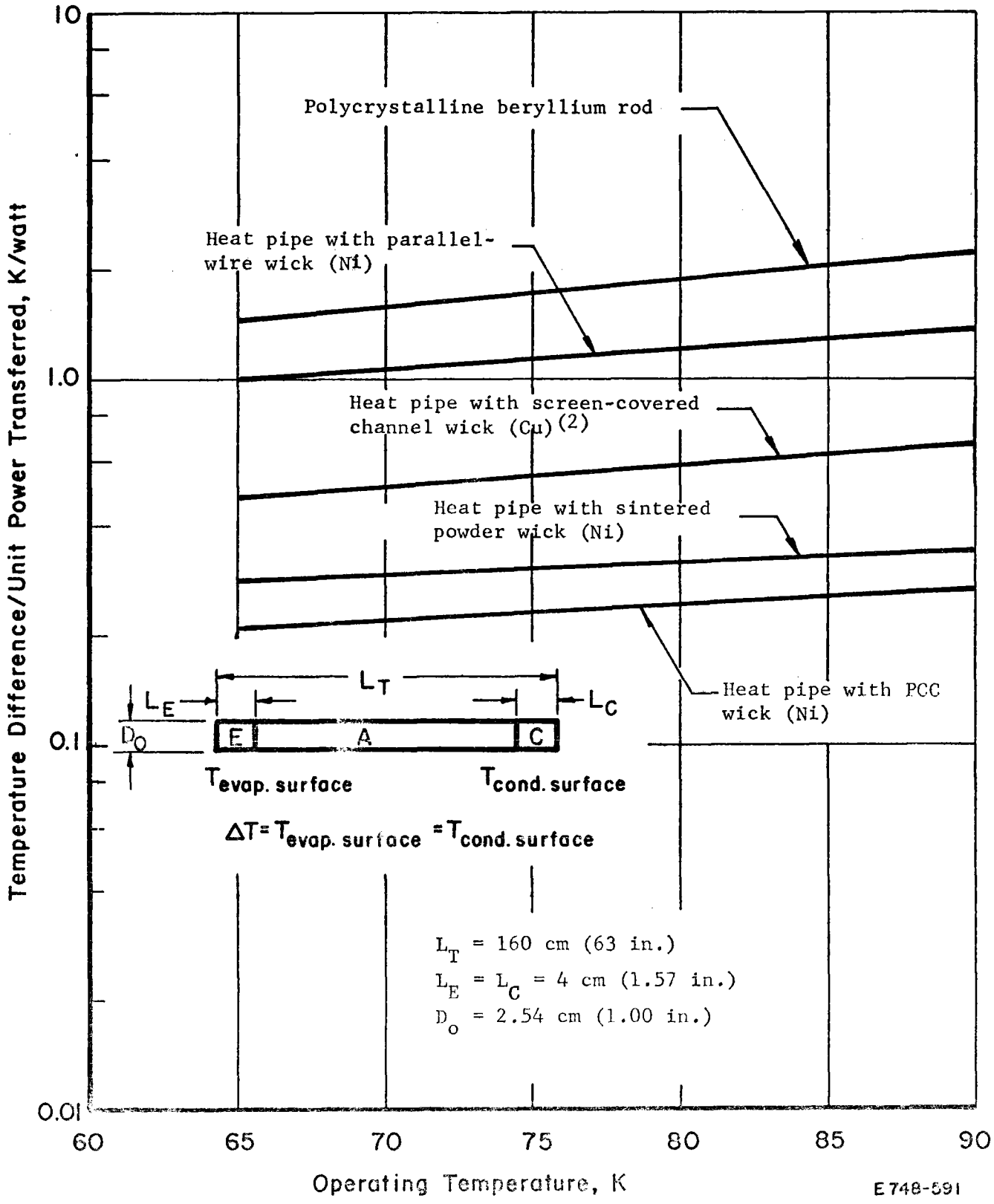

FIGURE 34. TEMPERATURE DIFFERENCE PER UNIT POWER TRANSFERRED FOR SELECTED WICK CONFIGURATIONS

SAMPLE INPUT/OUTPUT OF HEAT-PIPE COMPUTER PROGRAM

SAMPLE INPUT/OUTPUT OF HEAT-PIPE COMPUTER PROGRAM

Sample Input Data for LO_2 Heat Pipe

```
 5     T/C OF SLEEVE(WATTS/CM-C)
 10 1000.,0,0,0
 12 0,0,0,0
 13      T/C OF CONTAINER
 14 4.83714,-.00328,2.28571E-06,0
 16 0,0,0,0
 17     T/C OF WICK
 18 9.29188E-0[illegible],3.03257E-04,-4.33095E0[illegible]-05,0
 20 0,0,0,0
 21     LATENT HEAT(CAL/GRAM)
 22 1.6960600[illegible],-5.6916557E+0[illegible],1.0964801E-01,-9.4833523E-04
 24 2.993139
 24 2.9993139E-0[illegible],0,0,0
 25     VAPOR VISCOSITY(POISE)
 26 -2.2746292E-04,5.0751066E-0[illegible],-2.4675476E-08,4.336677E-11
 28 0,0,0,0
 29     LIQUID VISCOSITY(POISE)
 30 2.4342856E-03,-4.3559522E-0[illegible],3.1964284E-7,-6.5476184E-10
 32 0,0,0,0
 33     VAPOR PRESSURE(DYNES/CM**[illegible])
 34 6.0173540E+06,-4.1839264E+0[illegible],1.1006125E+04,-1.3005024E+02
 36 5.8350904E+[illegible]-01
 36 5.8350904E-01,0,0,0
 37     VAPOR DENSITY(GRAMS/CM**3)
 [illegible] 1.0666[illegible]E+00,-7.0614719E-02,1.6559566E-03,-8.4165024E-05
 40 1.5552083E-07,-3.9407443E-1[illegible],0,0
 41     LIQUID DENSITY(GRAMS/CM**3)
 42 -9.7[illegible]E+02,8.9524101E+01,-3.4811306E+00,7.4786866E-02
 44 -9.5371640E-04,7.3340368E-06,-3.1002187E-08,5.5866999E-11
 45     SPECIFIC HEAT RATIO(UNITLESS)
 46 1.125,0,0,0
 48 0,0,0,0
 49     SURFACE TENSION(DYNES/CM)
 50 -1.5900184E+01,1.7648407E+00,-2.3953442E-02,1.8166736E-03
 50 -1.5900184E+01,1.7648407E+00,-2.3953442E-02,1.8166736E-04
 52 -4.1666639E-07,0,0,0
```

Sample Output Data for LO_2 Heat Pipe

HEAT PIPE COMPUTER PROGRAM--PROGRAMMED BY PHILIP E. EGGERS
VERSION 1B , 3/10/70 , UPDATED BY J. T. ROBERTS

ARE FILE1 COEFFICIENTS DERRIVED FROM TEMPERATURES IN
DEGREES KELVIN,CENTIGRADE OR FAHRENHEIT

ENTER 'K' , 'C' OR 'F' ?K

DIMENSIONS FOR R'S AND Z'S IN CENTIMETERS

PHI= 0.10 RP= 1.27 RW= 1.19 RV= 0.650

ZE= 4.05 ZA= 152. ZC= 4.05

TEMP	GAMMA	RHO LIQ	RHO VAP	VIS LIQ	VIS VAP	PVAP
65.00	18.9.	1.26	.509E-04	.449E-02	.101E-04	.237E+05
75.00	17.0	1.22	.653E-03	.314E-02	.327E-04	.145E+06
85.00	14.7	1.17	.244E-02	.214E-02	.523E-04	.566E+06
95.00	12.2	1.12	.710E-02	.145E-02	.692E-04	.163E+07

LAMINAR FLOW REGIME

TEMP K	RAD. REN. NO. EVAP	COND	AXIAL REN. NO. EVAP	ADIABATIC	COND	ZMAX CM.
65.00	3091.04	3091.04	38499.5	38499.5	38499.5	6731.16
75.00	2989.60	2989.60	37236.0	37236.0	37236.0	8164.26
85.00	2279.63	2279.63	28393.2	28393.2	28393.2	7351.[illegible]
95.00	2024.84	2024.84	25219.6	25219.6	25219.6	6411.05

IS A PRINTOUT OF LAMINAR FLOW REGIME REQUESTED
?YES

TEMP	RC	DELTL	DELTLC	DELTP
K	CM.	K	K	PSI
65.00	0.002C0	42.C	42.0	.506E-02
75.00	0.00200	1[illegible]	125.	.401E-02
85.00	0.00200	1[illegible]	144.	.210E-02
95.00	0.00200	1[illegible]	159.	.112E-02

HEAT FLUXES FØR LAMINAR FLØW REGIME

TEMP K	DELTA T K	Q(SØNIC) WATTS	Q(ENTRN) WATTS	Q(WICK) WATTS	Q(BØIL) WATTS
65.00	84.00	362.3	185.7	454.4	4566771.9
75.00	250.79	3114.5	611.8	564.7	1837925.1
85.00	288.77	11417.4	1055.1	661.9	9223635.6
95.00	317.42	31442.8	1563.1	740.5	6908368.4

IS A PRINTØUT ØF TURBULENT FLØW REGIME REQUESTED
?YES

TURBULENT FLØW REGIME

TEMP K	RAD. REN. NØ. EVAP	RAD. REN. NØ. CØND	AXIAL REN. NØ. EVAP	AXIAL REN. NØ. ADIABATIC	AXIAL REN. NØ. CØND	ZMAX CM.
65.00	2675.94	2675.94	33329.3	33329.3	33329.3	8781.16
75.00	1901.24	1901.24	23680.3	23680.3	23680.3	8164.26
85.00	1704.16	1704.16	21225.6	21225.6	21225.6	7351.06
95.00	1657.93	1657.93	20649.8	20649.8	20649.8	6411.05

TEMP	RC	DELTLE	DELTLC	DELTP
K	CM.	K	K	PSI
65.00	0.00200	36.4	36.4	.111E-02
75.00	0.00200	79.7	79.7	.253E-03
85.00	0.00200	106.	108.	.110E-03
95.00	0.00200	130.	130.	.532E-04

HEAT FLUXES FØR TURBULENT FLØW REGIME

TEMP K	DELTA T K	Q(SØNIC) WATTS	Q(ENTRN) WATTS	Q(WICK) WATTS	Q(BØIL) WATTS
65.00	72.72	362.3	185.7	160.7	4566771.9
75.00	159.49	3114.5	611.8	359.1	1837925.1
85.00	215.87	11417.4	1055.1	494.8	-9223635.6
95.00	259.90	31442.8	1563.1	606.3	6908368.4

TEMP	DLTTVL	DLTTVT
65.00	0.528	0.116
75.00	0.937E-01	0.590E-02
85.00	0.168E-01	0.877E-03
95.00	0.410E-02	0.194E-03

HEAT PIPE BIBLIOGRAPHY

TABLE 4. HEAT PIPE BIBLIOGRAPHY

Theory

T. P. Cotter, "Heat Pipe Startup Dynamics", Thermionic Conversion Specialist Conference, Palo Alto, 1967.

D. Ernst, "Evaluation of Theoretical Heat Pipe Performance", Thermionic Conversion Specialist Conference, Palo Alto, 1967.

C. A. Busse, "Pressure Drop in the Vapor Phase of Long Heat Pipes", Thermionic Conversion Specialist Conference, Palo Alto, 1967.

J. Bohdansky, H. Strub, and E. van Andel, "Heat Transfer Measurements Using a Sodium Heat Pipe Working at Low Pressure", Thermionic Conversion Specialist Conference, Houston, 1966.

T. P. Cotter, "Theory of Heat Pipes", Los Alamos Scientific Laboratory Report LA-3246-MS, March 1965.

T. P. Cotter, "Status of Engineering Theory of Heat Pipes", Proceedings of Joint Atomic Energy Commission/Sandia Laboratories Heat Pipe Conference, AEC Research and Development Report SC-M-66-623, Sandia Corporation, Oct. 1966.

A. Carnesale, J. H. Cosgrove, and J. K. Terrell, "Operating Limits of the Heat Pipe", Proceedings of Joint Atomic Energy Commission/Sandia Laboratories Heat Pipe Conference, AEC Research and Development Report SC-M-66-623, Sandia Laboratories, Oct. 1966.

T. P. Cotter, J. Deverall, G. F. Erickson, G. M. Grover, E. S. Keddy, J. E. Kemme, and E. W. Salmi, "Status Report on Theory and Experiments on Heat Pipes at Los Alamos", Los Alamos Scientific Laboratory Report LADC-7206, 1965.

S. W. Yuan and A. B. Finkelstein, "Laminar Pipe Flow with Injection and Suction Through a Porous Wall", ASME Transactions, 78, pp 719-724, 1956.

Quarterly Status Report on the Space Electric Power R and D Program for the Period Ending January 31, 1968, Part I, "Los Alamos Scientific Laboratory Report LA-38881-MS, Feb. 21, 1968.

M. Armand and A. M. Schroff, "Resulat preliminaires d'une étude sur les caloducs a haute temperature", Second International Conference on Thermionic Electrical Power Generation, Stresa, Italy, 1968.

F. Reiss and K. Schretzmann, "Pressure Balance and Maximum Power Density at the Evaporation and Condensation Gained from Heat Pipe Experiments", Second International Conference on Thermionic Electrical Power Generation, Stresa, Italy, 1968.

G. B. Andeen, F. R. Kern, and P. Griffith, "Progress Report on Two-Phase Momentum Flux and Design of a Heat Pipe", MIT Contract AT(30-1)-3496, June 30, 1965.

W. A. Ranken and J. E. Kemme, "Survey of Los Alamos and EURATOM Heat Pipe Investigations", Thermionic Conversion Specialist Conference, San Diego, 1965.

S. W. Chi and T. A. Cygnarowicz, "Theoretical Analyses of Cryogenic Heat Pipes", submitted for presentation at the ASME 1970 Space Technology and Heat Transfer Conference, June 21-24, 1970, Los Angeles, California.

Applications

J. Deverall and E. Salmi, "Heat Pipe Performance in Space Environment", Thermionic Conversion Specialist Conference, Palo Alto, 1967.

W. E. Harbaugh and R. W. Longsderff, "The Development of an Insulated Thermionic Converter/Heat Pipe Assembly", Thermionic Conversion Specialist Conference, Houston, 1966.

P. K. Shefsiek, "Thermal Measurements on a Thermionic-Converter/Heat Pipe System", Thermionic Conversion Specialist Conference, Houston, 1966.

S. Katzoff, "Notes on Heat Pipes and Vapor Chambers and Their Application to Thermal Control of Spacecraft", Proceedings of Joint Atomic Energy Commission/ Sandia Laboratories Heat Pipe Conference, AEC Research and Development Report, Sandia Corporation, SC-M-66-623, Oct. 1966.

J. E. Deverall and J. E. Kemme, "Satellite Heat Pipe", Los Alamos Scientific Laboratory Report LA-3278-MS, Jan. 1965.

G. M. Grover, J. Bohdansky, C. A. Busse, "The Use of a New Heat Removal System in Space Thermionic Power Supplies", report EUR 2229.e (EURATOM) 1965.

C. A. Busse, R. Caron, and C. Cappelletti, "Prototypes of Heat Pipe Thermionic Converters for Space Reactors", Proc. Int. Conf. on Thermionic Electrical Power Generation, London, 1965.

"Quarterly Status Report on Advanced Reactor Technology (ART) for Period Ending July 31, 1967, Part I, "Los Alamos Scientific Laboratory Report LA-3760-MS, Aug. 1967.

J. E. Kemme, "Heat Pipe Capability Experiments", Thermionic Conversion Specialist Conference, Houston, 1966.

J. E. Deverall and J. E. Kemme, "Satellite Heat Pipe", Los Alamos Scientific Laboratory Report LA-3278-MS, Jan. 1965.

C. A. Busse, R. Caron, F. Geiger, M. Potzschke, "Performance Studies on Heat Pipes", Proc. Int. Conf. on Thermionic Electrical Power Generation, London, 1965.

J. Bohdansky and H.E.J. Schins, "Heat Transfer in Heat Pipe Operating at Emitter Temperatures", Int. Conf. on Thermionic Electrical Power Generation, London, 1965.

A. Carnesale, J. H. Cosgrove, and J. K. Terrell, "Operating Limits of the Heat Pipe", Proceedings of Joint Atomic Energy Commission/Sandia Laboratories Heat Pipe Conference, AEC Research and Development Report SC-M-66-623, Sandia Corporation, Oct. 1966.

T. P. Cotter, J. Deverall, G. F. Erickson, G. M. Grover, E. S. Keddy, J. E. Kemme, and E. W. Salmi, "Status Report on Theory and Experiments on Heat Pipes at Los Alamos", Los Alamos Scientific Laboratory Report LADC-7206, 1965.

G. H. Parker and J. P. Hanson, "Heat Pipe Analysis", Intersociety Energy Conversion Engineering Conference, Miami, 1967.

J. Deverall and J. Kemme, "High Thermal Conductance Devices Utilizing the Boiling of Lithium and Silver", Los Alamos Scientific Laboratory Report LA-3211, 1965.

L. S. Langston, A. Sherman, and B. H. Hilton, "Third Quarterly Report, Vapor Chamber Fin Studies", NASA CR-54989, PWA-2818; April 1966.

J. E. Deverall and E. W. Salmi, "Orbital Heat Pipe Experiment", Los Alamos Scientific Laboratory Report LA-3714, June 1967.

A. Bahr, E. Burk, and W. Hufschmidt, "Liquid-Vapors Interaction and Evaporation in Heat Pipes", Second International Conference on Thermionic Electrical Power Generation, Stresa, Italy, 1968.

R. Semeria and E. Schmidt, "Determination theorique et experimentale de la puissance therminque limitz transferre par des caloducs a sodium", Second International Conference on Thermionic Electrical Power Generation, Stresa, Italy, 1968.

G. H. Parker and J. P. Hanson, "Heat Pipe Analysis", Intersociety Energy Conversion Engineering Conference, Miami, 1967.

B. W. Knight and B. B. McInteer, "Laminar Incompressible Flow in Channels with Porous Walls", Los Alamos Scientific Laboratory Report LADC-5309.

W. E. Wageman and F. A. Guevara, "Fluid Flow Through a Porous Channel", Phys. Fluids 3, p 878 (1960).

J. H. Cosgrove, J. K. Ferrell, and A. Carnesale, "Operating Characteristics of Capillarity Limited Heat Pipes", J. Nuclear Energy 21, pp 547-558, 1967.

L. Langston and H. R. Kunz, "First Quarterly Report, Vapor Chamber Fin Studies", NASA-CR-54882; PWA-2688 (Sept. 1965).

S. Frank, "Optimization of a Grooved Heat Pipe", Intersociety Energy Conversion Engineering Conference, Miami, 1967.

T. P. Cotter, "Advances in Heat Pipe Theory", Second International Conference on Thermionic Power Generation, Stresa, Italy, 1968.

E. van Andel, "Heat Pipe Optimization", Second International Conference on Thermionic Electrical Power Generation, Stresa, Italy, 1968.

G. B. Andeen, F. R. Kern, and P. Griffith, "Progress Report on Two-Phase Momentum Flux and Design of a Heat Pipe", MIT Contract AT(30-1)-3496, June 30, 1965.

M. Schindler and G. Woessner, "Theoretisches Model zum Waermetransport in Waermeuebertragungsrohren", (Theoretical Considerations on Heat Transfer in Heat Pipes) Atomkern Energie, 10:395-398(Sept.-Oct. 1965).

G. B. Andeen, F. R. Kern, and P. Griffith, "Progress Report on Two Phase Momentum Flux and Design of a Heat Pipe", MIT Contract AT(30-1)-3496, June 30, 1965.

B. Shelpuk, et al, "ICICLE - An Integrated Cryogenic Isotope Cooling Engine System", submitted for presentation at the ASME 1970 Space Technology and Heat Transfer Conference, June 21-24, 1970, Los Angeles, California.

Performance

J. Kemme, "High Performance Heat Pipes", Thermionic Conversion Specialist Conference, Palo Alto, 1967.

J. Deverall and E. Salmi, "Heat Pipe Performance in Space Environment", Thermionic Conversion Specialist Conference, Palo Alto, 1967.

J. Bohdansky, H. Strub, and E. van Andel, "Heat Transfer Measurements Using a Sodium Heat Pipe Working at Lower Vapor Pressure", Thermionic Conversion Specialist Conference, Houston, 1966

"Quarterly Status Report on Advanced Reactor Technology (ART) for Period Ending July 31, 1967, Part I", Los Alamos Scientific Laboratory Report LA-3760-MS, August 1967.

H. C. Haller and S. Lieblein, "Feasibility Studies of Space Radiators Using Vapor Chamber Fins", Proceedings of Joint Atomic Energy Commission/Sandia Laboratories Heat Pipe Conference, AEC Research and Development Report SC-M-66-623, Sandia Corporation, Oct. 1966.

C. A. Busse, "Optimization of Heat Pipe Thermionic Converters for Space Power Supplies", EURATOM report ERU 2534.e.

J. Bohdansky and H. E. J. Schins, "A New Method for Vapor Pressure Measurements at High Temperature and High Pressure", J. Appl. Phys. 55.

P. Brosens, "Thermionic Converters with Heat Pipe Radiators", Intersociety Energy Conversion Engineering Conference, Miami, 1967.

J. E. Deverall and E. W. Salmi, "Orbital Heat Pipe Experiment", Los Alamos Scientific Laboratory Report LA-3714, June 1967.

W. E. Harbaugh, "The Development of an Insulated Thermionic Converter-Heat Pipe Assembly", Radio Corporation of America, Technical Report AFAPL-TR-67-45, April 1967.

Wick Structure

J. E. Kemme, "Heat Pipe Capability Experiments", Thermionic Conversion Specialist Conference, Houston, 1966.

S. Katzoff, "Notes of Heat Pipes and Vapor Chambers and Their Application to Thermal Control of Spacecraft", Proceedings of Joint Atomic Energy Commission/ Sandia Laboratories Heat Pipe Conference, AEC Research and Development Report, Sandia Corporation, SC-M-66-623, Oct. 1966.

H. R. Kunz, L. S. Langston, B. H. Hilton, S. S. Wyde, and G. H. Nashick Washington, "Vapor-Chamber Fin Studies, Transport Properties and Boiling Characteristics of Wicks", Pratt and Whitney Aircraft Report NASA-CR-812, PWA-20531 June 1967.

L. S. Langston, A. Sherman, and B. H. Hilton, "Vapor-Chamber Fin Studies, Third Quarterly Report", Pratt and Whitney Aircraft Report NASA-CR-54-989, PWA-2818, April 1966.

L. S. Langston, A. Sherman, and B. H. Hilton, "Vapor-Chamber Fin Studies, Second Quarterly Report", Pratt and Whitney Aircraft Report NASA-CR-54922, PWA-2773, Jan. 1966.

L. Langston and H. R. Kunz, "Vapor Chamber Fin Studies, First Quarterly Report", Pratt and Whitney Aircraft Report NASA-CR-54882; PWA-2698, Sept. 1965.

"Quarterly Status Report on the Space Electric Power R and D Program for the Period Ending January 31, 1968, Part I", Los Alamos Scientific Laboratory Report LA-3881-MS, Feb. 31, 1968.

"Quarterly Status Report on Advanced Reactor Technology (ART) for Period Ending July 31, 1967, Part I", Los Alamos Scientific Laboratory Report LA-3760-MS, Aug. 1967.

Corrosion

C. A. Busse, F. Geiger, M. Potzschke, D. Quataert, "Heat Pipe Lifetests at 1600 C and 1000 C", Thermionic Conversion Specialist Conference, Houston, 1966.

C. A. Busse, F. Geiger, H. Strub, and M. Potzschke, "High Temperature Lithium Heat Pipes", Second International-Conference on Thermionic Electrical Power Generation, Stresa, Italy, 1968.

W. A. Ranken and J. E. Kemme, "Survey of Los Alamos and EURATOM Heat Pipe Investigations", Thermionic Conversion Specialist Conference, San Diego, 1965.

C. A. Busse, R. Caron, F. Geiger, and M. Potzschke, "Performance Studies on Heat Pipes", Proceedings International Conference on Thermionic Electrical Power Generation, London, 1965.

"Quarterly Status Report on the Space Electric Power R and D Program for the Period Ending January 31, 1968, Part I", Los Alamos Scientific Laboratory Report LA-3881-MS, Feb. 31, 1968.

Cryogenic Heat Transfer and Containment

R. J. Balthazar, et al, "The Development of Titanium and Inconel Cryogenic Pressure Vessels", Advances in Cryogenic Engineering, Vol 11, pages 437-446 (1966).

C. G. Fritz, "A Study of Bubble Motion in Liquid Nitrogen", ibid, pages 584-592.

D. S. Dillard, et al, "Thermal Transport Properties of Selected Solids at Low Temperatures," Advances in Cryogenic Heat Transfer, pages 1-20 (1968).

D. N. Lyon, "Pool Boiling of Cryogenic Liquids", ibid, pages 82-92.

J. A. Clark, "Gravic and Agravic Effects in Cryogenic Heat Transfer", ibid, pages 93-102.

C. B. Cobb, "Correlation of the Maximum Heat Flux and Temperature Difference in the Nucleate Boiling of Corresponding States Liquids", Advances in Cryogenic Engineering, Vol 12, pages 381-386 (1966).

General and Miscellaneous

G. M. Grover, T. P. Cotter, and G. F. Erickson, "Structures of Very High Thermal Conductances", J. Appl. Phys. 35, 1990 (1964).

W. A. Ranken and J. E. Kemme, "Survey of Los Alamos and EURATOM Heat Pipe Investigations", Thermionic Conversion Specialist Conference, San Diego, 1965.

K. T. Feldman, Jr. and G. H. Whiting, "The Heat Pipe", Mechanical Engineering (Feb. 1967).

F. Reiss and K. Schretzmann, "The Axial Heat Power Distribution in Inductively Heated Tubes", Second International Conference on Thermionic Electrical Power Generation, Stresa, Italy, 1968.

Philip E. Eggers

Project Leader, Materials Systems Engineering Division
B.S., physics (1963) The Ohio State University
M.S., physics (1966) The Ohio State University

Mr. Eggers joined the Battelle staff in 1963 where he became engaged in the development of improved laser microprobes, and participated in the successful development of a thermally activated energy cell. In addition, he has participated in studies of thermoelectric applications for space generator design, including formulating a computer code to obtain thermoelectric materials performance data. He has also written a generator weight analysis computer code to permit the minimum weight optimization of thermoelectric generators, and has been engaged in (1) a segmented thermoelectric research and development program, particularly the measurement of elevated-temperature contact resistivity of semiconductor-metal junctions, and (2) the study of the effects of neutron irradiation on the yield strength of metals using multiple regression analysis techniques, and (3) the study of heat transfer problems associated with "grinding" operations.

Mr. Eggers has acquired considerable experience in the theoretical analysis, experimental testing, and design/fabrication of heat pipes. Mr. Eggers has been principal investigator in a previous government-sponsored heat-pipe program (April, 1969, to September, 1969), and has designed and developed specialized test apparatus for charging and testing of heat pipes.

Mr. Eggers is currently in charge of a program for NASA where development of an advanced concept for energy conversion is being studied, as well as the development of measurement techniques for characterizing thermoelectric materials and evaluating thermoelectric components. Also, he is presently in charge of a BCL-funded experimental study of advanced heat-pipe concepts.

Prior to joining Battelle, Mr. Eggers spent three summers at the B.F. Goodrich Research Center performing experimental studies of gas diffusion and polymerization. In this study of gas diffusion, an elastomeric material with low permeability to refrigerant gases was successfully developed.

Mr. Eggers is presently studying toward the degree of Doctor of Philosophy in the field of solid-state physics at The Ohio State University. He is a member of Ther American Physical Society, Ohio Academy of Sciences, American Association for the Advancement of Science, American Society for Testing and Materials, and Sigma Pi Sigma (national physics honor society).

Publication of technical papers have included the areas of (1) design optimization of thermoelectric generators, (2) studies of the effects of neutron irradiation on mechanical properties of single crystal and polycrystalline metals, (3) development of advanced testing techniques for evaluating thermoelectric components, and (4) design, fabrication, and evaluation of small-diameter heat pipes for operation in ambient temperature regime (to be published).